Uncertain dynamic analysis for rigid-flexible mechanisms with random geometry and material properties

Jinglai Wu[a, *]

jinglai.wu@uts.edu.au

Zhen Luo[a]

Nong Zhang[a, *]

nong.zhang@uts.edu.au

Yunqing Zhang[b]

Paul D. Walker[a]

[a]School of Electrical, Mechanical and Mechatronic Systems, The University of Technology, Sydney, NSW 2007, Australia

[b]State Key Laboratory of Digital Manufacturing Equipment and Technology, School of Mechanical Science and Engineering, Huazhong University of Science and Technology, Wuhan, Hubei 430074, China

*Corresponding author.

Abstract

This paper proposes an uncertain modelling and computational method to analyze dynamic responses of rigid-flexible multibody systems (or mechanisms) with random geometry and material properties. Firstly, the deterministic model for the rigid-flexible multibody system is built with the absolute node coordinate formula (ANCF), in which the flexible parts are modeled by using ANCF elements, while the rigid parts are described by ANCF reference nodes (ANCF-RNs). Secondly, uncertainty for the geometry of rigid parts is expressed as uniform random variables, while the uncertainty for the material properties of flexible parts is modeled as a continuous random field, which is further discretized to Gaussian random variables using a series expansion method. Finally, a non-intrusive numerical method is developed to solve the dynamic equations of systems involving both types of random variables, which systematically integrates the deterministic generalized-α solver with Latin Hypercube sampling (LHS) and Polynomial Chaos (PC) expansion. The benchmark slider-crank mechanism is used as a numerical example to demonstrate the characteristics of the proposed method.

Keywords: Rigid-flexible multibody systems; Absolute node coordinate formula (ANCF); Random uncertainty; Polynomial Chaos (PC) expansion

1 Introduction

As one of the most important systems in mechanical engineering, almost all the multibody dynamic mechanical systems (or mechanisms) involve various uncertain factors, which may influence the performance of a system especially for the high-speed dynamic systems. For instance, the geometry size of a component in the mechanism has a tolerance to facilitate manufacturing process; the fabrication of different kinds of raw material may lead to the inhomogeneous distribution of the material, which will further lead to the variation of material properties, such as the Young's modulus, Poisson's ratio, and material density. To improve the computational accuracy of dynamic analysis of the mechanism, it is necessary to investigate their dynamic responses by considering these unavoidable uncertain factors.

The dynamic study of the mechanisms under deterministic conditions has been developed from traditional rigid multibody systems to flexible multibody systems and rigid-flexible multibody systems. The modelling of rigid multibody systems has been well studied [1], and some commercial software has also been widely used. On the other hand, the study of flexible multibody systems and rigid-flexible multibody systems has been attracting more and more attention over the past two decades. When the flexible components are involved in multibody systems, the deformation of these flexible components has to be considered. Since flexible components in multibody systems often experience large rotation and deformation, the traditional finite element methods based on the small rotation and deformation may give an improper solution [2]. However, the Absolute Nodal Coordinate Formulation (ANCF) [3] shows good capability for solving flexible multibody problems with large rotation and deformation. ANCF defines elemental coordinates as the absolute displacements and global slopes, which forces the mass matrix of the system equations to remain constant and the centrifugal and Coriolis forces identically equal to zero [4,5]. As a non-incremental finite

element method, the ANCF has been considered as an effective approach for analysis of flexible multibody dynamics [6]. There have been some applications with the flexible multibody systems solved by using the ANCF, such as the flexible multibody systems with viscoelastic materials [7], the clearance and lubricated joints problems [8], and large deformation problems [9–12].

To solve the rigid-flexible multibody systems, Tian et al. [13] combined ANCF with Natural Coordinate Formulation (NCF) to build dynamic models of rigid-flexible multibody systems, in which the flexible parts were modeled by using ANCF elements and the rigid parts were described by the NCF. Liu et al. [14] used the ANCF-NCF method to compute the dynamic response of a large scale rigid-flexible multibody system composed of composite laminated plates. Similar to the concept of NCF, Shabana [15] employed the ANCF reference nodes (ANCF-RNs) to describe the rigid body. As a result, the complicated rigid-flexible multibody systems could be modeled by using the ANCF-based method, in which the flexible parts were built by the ANCF elements while the rigid parts were described by the ANCF-RNs. More applications about the ANCF-based method on the rigid-flexible multibody systems can be found in [16].

To solve the multibody systems containing uncertain parameters, not only the aforementioned deterministic methods but also some uncertain analysis methods have to be used. Based on the different characteristics of uncertain parameters, the uncertain analysis methods can be divided into two categories, which are the probabilistic methods to solve the random parameters and the non-probabilistic methods to solve other non-probabilistic parameters [17,18]. Non-probabilistic methods [19–25] are mainly used as a complimentary of probabilistic methods when the probabilistic information of uncertain parameters may not be obtained. There also have been some references focusing on the hybrid uncertain methods [26,27].This paper is focused on the probabilistic methods by assuming the characteristics of random parameters are known.

In a rigid-flexible multibody system, the uncertain parameters of the rigid parts may be directly described by random variables, e.g. the mass, mass center, mass moment of inertia, and geometry size. Specifically, the geometry size is certainly subject to uncertainty for the tolerance of manufacture, and it will lead to the uncertainty of other parameters, e.g. mass center, mass, mass moment of inertia, gravity force, and constraint conditions. On the other hand, the inhomogeneous distribution of material in space may result in uncertainty of material properties (e.g. Young's modulus and Poisson's ratio), which may continuously vary. Therefore, the uncertainties of material properties should be described as random fields. The random field has been widely used in structure analysis [28–30], but it is rarely used in the dynamic computation of multibody systems.

The continuous random field is defined as an indexed set of random variables, and the index belongs to some continuous uncountable set. Since the uncountable index set is not convenient to implement in the computation, the random field needs to be discretized into a set of countable random variables. Ghanem and Spanos [30] has stated that a continuous random field can be approximately represented by a set of countable random variables. The most widely used discretization methods for the random field are series expansion methods, which aim at expanding any realization of the original random field over a complete set of deterministic functions [31]. After the series is obtained, the discretization is implemented by truncating the series after a finite number of terms. Karhunen-Loeve (K-L) expansion [30], orthogonal series expansion (OSE) [32], and expansion optimal linear estimation (EOLE) method [33] all belong to the series expansion methods. The K-L expansion method has the highest discretization accuracy, but only few covariance functions (e.g. the exponential autocorrelation function) have a closed-form solution for K-L expansion. Numerical methods have to be used to realize the K-L expansion, which can be found in references [29,30]. However, the orthogonal basis of the expansion obtained by most of the numerical methods is no more optimal [31]. The EOLE can be considered as a special case of the Nystrom method that is a type of numerical method to implement the K-L expansion [29], and it is based on an optimal basis. The paper [31] gave a comparison of the discretization methods and indicated that the EOLE could be used in more general cases with high accuracy.

After the discretization, the uncertain material properties of the flexible parts have been transformed to several random variables, the same as other random parameters in the rigid parts. At this stage, the key is to obtain the uncertain characteristics of response (output) from the input random variables, which is the about uncertainty propagation of the random variables. The statistical method [34] is the first strategy to handle this problem, which collects a large number of samples of the random variables according to their probability distribution and then estimates the mean, variance, and even the probability distribution function of the output directly. The Monte Carlo method [35] is one important statistical method, but its accuracy depends on the sampling size, in accordance with the weak law of large numbers. Therefore, to get sufficient accuracy, it usually requires thousands of samples, which is quite expensive for the dynamic computation of rigid-flexible multibody systems. As a result, the Monte Carlo method is often used as the reference of other methods. The samples of Monte Carlo method are produced randomly, some other sampling strategies can be used to improve the convergence ratio of Monte Carlo method, such as the Latin Hypercube sampling (LHS) [36], Orthogonal Sampling [37], low discrepancy sampling [38] and so on [39]. This paper will use the LHS method to improve the convergence ratio of statistical method.

Non-statistical methods [34] can also be used to handle the random variables, e.g. the perturbation method, Neumann expansion method, and Polynomial Chaos (PC) expansion method [40]. These methods can be regarded as a kind of surrogate model-based methods, in which the perturbation method and Neumann expansion method are more like the low-order polynomials. They require the uncertainty extent of random variables to be small. The PC expansion method approximates the response of system by a truncated orthogonal series and then uses the characteristics of orthogonal polynomials to estimate the first and second

moment of the random response. The PC expansion can be regarded as a type of high-order polynomials model. It can be used to handle the random variables with relatively larger uncertainty. The PC expansion method has been widely used, such as in fluid mechanics [41], vehicle dynamics [42,43], multibody dynamic systems [44–46], structure dynamics [47], optimization problems [48], and hybrid uncertainties [27,49]. One weakness for the PC expansion is the dimensional curse problem, so that it may not be suitable for the high dimensional problems. Another problem for the PC expansion is that its accuracy strongly depends on the smooth extent of the system responses, so it may be not efficient for the rigid-flexible multibody systems which contain many high frequency responses, which will be discussed in Section 5.

The paper investigates the dynamic response of the rigid-flexible mechanisms containing both geometry and material uncertainties which are modeled by random variables and random field. A non-intrusive numerical method, which systematically integrates the ANCF, discretization of random field, solver of DAEs, statistical and PC expansion methods will be proposed. Some guidelines about their applications in the rigid-flexible multibody systems will also be provided.

2 ANCF-based method for solving the rigid-flexible multibody system

2.1 The ANCF-based element and ANCF-RN

This paper studies the planar mechanism, so we just briefly review the two-dimensional ANCF beam elements, and more other ANCF elements can be found in references [5,12,50–52]. Fig. 1 shows the planar shear deformable beam element, where the X-Y denotes the global coordinate system.
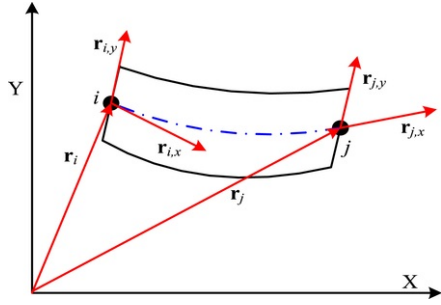

Fig. 1 Two dimensional ANCF beam element.

alt-text: Fig. 1

The displacement field of the element can be defined in the global coordinate system as

$$\mathbf{r} = \begin{bmatrix} r_1 & r_2 \end{bmatrix}^{\mathrm{T}} = \mathbf{Se}, \quad \mathbf{e} = \begin{bmatrix} \mathbf{e}_i^{\mathrm{T}} & \mathbf{e}_j^{\mathrm{T}} \end{bmatrix}^{\mathrm{T}} = \begin{bmatrix} \mathbf{r}_i^{\mathrm{T}} & \mathbf{r}_{i,x}^{\mathrm{T}} & \mathbf{r}_{i,y}^{\mathrm{T}} & \mathbf{r}_j^{\mathrm{T}} & \mathbf{r}_{j,x}^{\mathrm{T}} & \mathbf{r}_{j,y}^{\mathrm{T}} \end{bmatrix}^{\mathrm{T}} \quad (1)$$

where $\mathbf{r}$ denotes the nodal coordinates in the global coordinate system, $\mathbf{S}$ is the shape function of the element, $\mathbf{e}$ denotes the absolute nodal coordinate vector of node i and j, $\mathbf{r}_p$ ($p=i, j$) is the position coordinates defined in the global coordinate system, $\mathbf{r}_{p,x}$ is the derivative of $\mathbf{r}_p$ with respect to local coordinate x, and $\mathbf{r}_{p,y}$ is its derivative with respect to y.

The rigid parts are described by the ANCF-RNs [15], where the two-dimensional ANCF-RNs are shown as Fig. 2. The X-Y and X^k-Y^k are the global coordinate system and local coordinate system, respectively. The absolute coordinate vector of node k in ANCF-RNs is defined as

$$\mathbf{e}_k = \begin{bmatrix} \mathbf{r}_k^{\mathrm{T}} & \mathbf{r}_{k,x}^{\mathrm{T}} & \mathbf{r}_{k,y}^{\mathrm{T}} \end{bmatrix}^{\mathrm{T}} \quad (2)$$
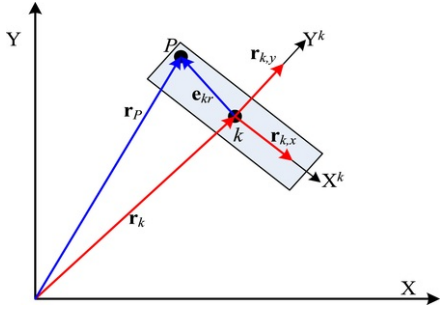
Fig. 2 Two dimensional ANCF-RNs.

alt-text: Fig. 2

Similar to the ANCF element, $\mathbf{r}_k$ is the position coordinates of node k defined in the global coordinate system, $\mathbf{r}_{k,x}$ and $\mathbf{r}_{k,y}$ are two vectors paralleling to the local coordinate axes X^k and Y^k, respectively. To describe a rigid body in two-dimensional space by the ANCF-RNs, the following three constraint equations should be added

$$\left\|\mathbf{r}_{k,x}\right\| = 1, \quad \left\|\mathbf{r}_{k,y}\right\| = 1, \quad \mathbf{r}_{k,x} \cdot \mathbf{r}_{k,y} = 0 \qquad (3)$$

Based on the Fig. 2, any point P on the rigid body can be expressed by the following equation

$$\mathbf{r}_P = \mathbf{r}_k + \mathbf{e}_{kr} = \mathbf{r}_k + \begin{bmatrix} \mathbf{r}_{k,x} & \mathbf{r}_{k,y} \end{bmatrix} \begin{bmatrix} x & y \end{bmatrix}^{\mathrm{T}} = \begin{bmatrix} \mathbf{I}_2 & x\mathbf{I}_2 & y\mathbf{I}_2 \end{bmatrix} \begin{bmatrix} \mathbf{r}_k^{\mathrm{T}} & \mathbf{r}_{k,x}^{\mathrm{T}} & \mathbf{r}_{k,y}^{\mathrm{T}} \end{bmatrix}^{\mathrm{T}} = \mathbf{S}_r \mathbf{e}_k \qquad (4)$$

where $\mathbf{e}_{kr}$ is the local position coordinate vector of point P, x and y are the local coordinates, $\mathbf{I}_2$ is the 2 by 2 unit matrix, and $\mathbf{S}_r$ denotes the shape function of the rigid body. It can be found that the position coordinates of points on the rigid body are expressed by the same formula as the ANCF element, but their shape functions are different.

2.2 Dynamic equations of the rigid-flexible multibody system

The nodal coordinates $\mathbf{e}$ can be transformed into the generalized coordinates $\mathbf{q}$ of a rigid-flexible multibody system. The equations of motion for a constrained rigid-flexible multibody system can be expressed in a compact form of the differential algebraic equations (DAEs) [4] as

$$\begin{cases} \mathbf{M}\ddot{\mathbf{q}} + \mathbf{\Phi}_{\mathbf{q}}^{\mathrm{T}}\boldsymbol{\lambda} + \mathbf{F}(\mathbf{q}) = \mathbf{Q}(\mathbf{q}) \\ \mathbf{\Phi}(\mathbf{q}, t) = \mathbf{0} \end{cases} \qquad (5)$$

where $\mathbf{M}$ is the system mass matrix, $\mathbf{\Phi}(\mathbf{q}, t)$ is the vector that contains the system constraint equations corresponding to the ideal joints, t represents the time, $\mathbf{\Phi}_{\mathbf{q}}$ is the derivative matrix of constraint equations with respect to the system generalized coordinates $\mathbf{q}$, $\boldsymbol{\lambda}$ is the Lagrangian multipliers associated with the constraints, $\mathbf{Q}(\mathbf{q})$ is the system external generalized forces, e.g. the gravity force, other external spring force and damping force, and $\mathbf{F}(\mathbf{q})$ denotes the system elastic force vector.

The mass matrix is composed of element mass matrix and the mass matrix of rigid bodies, which are constant and can be computed by the following equation

$$\mathbf{M}_e = \int_{V_e} \rho_e \mathbf{S}^{\mathrm{T}} \mathbf{S} dV_e, \quad \mathbf{M}_r = \int_{V_r} \rho_r \mathbf{S}_r^{\mathrm{T}} \mathbf{S}_r dV_r \qquad (6)$$

Here $\mathbf{M}_e$ is the element mass matrix, $\mathbf{M}_r$ denotes the rigid body mass matrix, ρ_e and ρ_r is the density of element in flexible parts and rigid body respectively, V_e denotes the volume of element, and V_r is the volume of rigid body.

The system elastic force $\mathbf{F}(\mathbf{q})$ is composed of element elastic force $\mathbf{F}_e$, which is computed by the following formula [53]

$$\mathbf{F}_e = -\mathbf{K}(\mathbf{e})\mathbf{e} = -\left(\mathbf{K}_1 + \mathbf{K}_2(\mathbf{e})\right)\mathbf{e} \qquad (7)$$

where the nonlinear stiffness matrix $\mathbf{K}(\mathbf{e})$ is the summation of a constant stiffness matrix $\mathbf{K}_1$ and another nonlinear stiffness matrix $\mathbf{K}_2(\mathbf{e})$ which is depend on the generalized coordinates. The constant stiffness matrix of the element is expressed by

$$\mathbf{K}_1 = -(\kappa + G)\int_V \sum_{\alpha=1}^{2} \mathbf{S}_{,\alpha}^{\mathrm{T}} \mathbf{S}_{,\alpha} dV \tag{8}$$

where the G denotes the Young's modulus, and κ is the Poisson's ratio. The entry of nonlinear stiffness matrix $\mathbf{K}_2(\mathbf{e})$ can be computed by

$$\left[\mathbf{K}_2(\mathbf{e})\right]_{ij} = \mathbf{e}^{\mathrm{T}} \mathbf{C}_{\mathbf{K}_2}^{ij} \mathbf{e} \tag{9}$$

where the $\mathbf{C}_{\mathbf{K}_2}^{ij}$ is a constant matrix, termed as invariant matrix [53], which is expressed as

$$\mathbf{C}_{\mathbf{K}_2}^{ij} = \frac{\kappa + 2G}{2}\sum_{\alpha=1}^{2}\int_{V_e}\left(\mathbf{S}_{,\alpha}^{\mathrm{T}}\mathbf{S}_{,\alpha}\right)_i^{T}\left(\mathbf{S}_{,\alpha}^{\mathrm{T}}\mathbf{S}_{,\alpha}\right)_j dV_e + \frac{\kappa}{2}\sum_{\alpha=1}^{2}\sum_{\beta=1,\beta\neq\alpha}^{2}\int_{V_e}\left(\mathbf{S}_{,\alpha}^{\mathrm{T}}\mathbf{S}_{,\alpha}\right)_i^{T}\left(\mathbf{S}_{,\beta}^{\mathrm{T}}\mathbf{S}_{,\beta}\right)_j dV_e + G\sum_{\alpha=1}^{2}\sum_{\beta=1,\beta\neq\alpha}^{2}\int_{V_e}\left(\mathbf{S}_{,\alpha}^{\mathrm{T}}\mathbf{S}_{,\beta}\right)_i^{T}\left(\mathbf{S}_{,\alpha}^{\mathrm{T}}\mathbf{S}_{,\beta}\right)_j dV_e \tag{10}$$

It should be noted that all the parameters in the above equations are considered as constant in deterministic case.

Several numerical methods can be used to solve the DAEs shown in Eq. (5), which can be found in the literature [54]. The generalized-$\boldsymbol{\alpha}$ method [55] will be used in this paper, since it has a good trade-off between the numerical accuracy at low-frequency and numerical damping at high-frequency. In the algorithm, the Eq. (5) is firstly discretized to the following algebraic equations at each time step, and then the Newton iteration is employed to solve the algebraic equations.

$$\mathbf{G}\left(\mathbf{q}_{i+1}, \boldsymbol{\lambda}_{i+1}\right) = \begin{bmatrix} \mathbf{M}\ddot{\mathbf{q}}_{i+1} + \boldsymbol{\Phi}_{\mathbf{q}}^{\mathrm{T}}\boldsymbol{\lambda}_{i+1} + \mathbf{F}\left(\mathbf{q}_{i+1}\right) - \mathbf{Q}\left(\mathbf{q}_{i+1}\right) \\ \boldsymbol{\Phi}\left(\mathbf{q}_{i+1}, t_{i+1}\right) \end{bmatrix} = \mathbf{0} \tag{11}$$

where

$$\begin{cases} \mathbf{q}_{i+1} = \mathbf{q}_i + h\dot{\mathbf{q}}_i + h^2\left(1/2 - \beta\right)\mathbf{a}_i + h^2\beta\mathbf{a}_{i+1} \\ \dot{\mathbf{q}}_{i+1} = \dot{\mathbf{q}}_i + h\left(1 - \eta\right)\mathbf{a}_i + h\eta\mathbf{a}_{i+1} \end{cases} \tag{12}$$

Here the subscript i denotes the ith time step, h is the step size, and $\mathbf{a}$ is the a new generalized vector that is determined by following equations

$$\mathbf{a}_0 = \ddot{\mathbf{q}}_0; \ \left(1 - \alpha_m\right)\mathbf{a}_{i+1} + \alpha_m\mathbf{a}_i = \left(1 - \alpha_f\right)\ddot{\mathbf{q}}_{i+1} + \alpha_f\ddot{\mathbf{q}}_i \tag{13}$$

The β, η, α_m, and α_f are the parameters in the generalized-$\boldsymbol{\alpha}$ algorithm. More detailed iteration procedure of the generalized-$\boldsymbol{\alpha}$ algorithm can be found in the reference [55].

3 Expression of random uncertain parameters

3.1 Uncertain geometry size of rigid body

The geometry size is the main uncertain source of the rigid body. The tolerance of components will make the geometry of a rigid body uncertain, so the geometry size of each component manufactured by the same process is still different. However, it is subject to change within a given interval (tolerance range). We can obtain the probability distribution information of geometry size by sampling a large number of components, and then it can be expressed by the random variables.

In this study, the uncertain geometry size is assumed to satisfy the uniform distribution. Using the symbol $\mathbf{E}\sim U[-1,1]^k$ to represent a vector with k independent standard uniform distribution random variables, the volume of the rigid body is rewritten as $V_i(\mathbf{E})$. Based on the definition, the system mass matrix (defined as Eq. (6)) depends on the volume of the rigid body, so it will be expressed by the random variables $\mathbf{E}$. At the same time, the system generalized external forces, e.g. the gravity force for this paper, depends on the system mass matrix, so it is also expressed by the random variables $\mathbf{E}$. On the other hand, some constraints also depend on the geometry size. Therefore, they will be expressed by a function of the random variables as

$$\mathbf{M} = \mathbf{M}(\mathbf{E}), \mathbf{Q}(\mathbf{q}) = \mathbf{Q}(\mathbf{q}, \mathbf{E}), \boldsymbol{\Phi}(\mathbf{q}, t) = \boldsymbol{\Phi}(\mathbf{q}, \mathbf{E}, t) \tag{14}$$

In the dynamic analysis, the previous three parameters are changed with the random variables. We can sample the random variables with different values to compute these parameters (e.g. by using Eq. (6)) and then submit them into Eq. (11) to solve the system.

3.2 Uncertain material properties of flexible body

The material properties are the important uncertain factors of the flexible body. Being different from the geometry size, the material properties of the flexible body may change in the space domain, so they need to be described

by the random field. The random field may be thought as a giant laboratory where an investigator can do numerous experiments. The location of each experimental setup in the laboratory is identified, in the terminology of random fields, by a set of coordinates or parameters [56]. For the d-dimensional space, locations are denoted by a vector $\mathbf{x} \in \mathbf{D}$, where $\mathbf{D}$ is an open set of R^d describing the system geometry. When $d=1$, the random field is called as univariate random field which is also termed as random process. Therefore, a random field $Y(\mathbf{x}, \theta)$ can be defined as a curve in $\mathbf{L}^2(\Omega, \mathbf{F}, \mathbf{P})$, that is a collection of random variables indexed by the continuous parameter $\mathbf{x}$. This means that for a given $\mathbf{x}_0$, $Y(\mathbf{x}_0, \theta)$ is a random variable. Conversely, for a given outcome θ_0, $Y(\mathbf{x}, \theta_0)$ is a realization of the field [31].

The values of a random field at different locations are not independent, and their dependence is described by the covariance function C or correlation function $\widetilde{\rho}$. For a random field $Y(\mathbf{x}, \theta)$, its covariance function and correlation function are defined as follows

$$C\left(\mathbf{x}_1, \mathbf{x}_2\right) \equiv \text{Cov}\left[Y\left(\mathbf{x}_1, \theta\right), Y\left(\mathbf{x}_2, \theta\right)\right], \widetilde{\rho}\left(\mathbf{x}_1, \mathbf{x}_2\right) \equiv \frac{C\left(\mathbf{x}_1, \mathbf{x}_2\right)}{\sigma\left(\mathbf{x}_1\right) \sigma\left(\mathbf{x}_2\right)} \tag{15}$$

where Cov[f, g] denotes the covariance of random variables f and g, $\sigma(\mathbf{x}_i)$ is the standard deviation of random variable $Y(\mathbf{x}_i, \theta)$.

The random field is a Gaussian field if any vector $[Y(\mathbf{x}_1, \theta) \ ... \ Y(\mathbf{x}_{q}, \theta)]^{\text{T}}$ is Gaussian. The Gaussian field is completely defined by its mean $\mu(\mathbf{x}, \theta)$, variance $\sigma^2(\mathbf{x}, \theta)$ and correlation functions $\widetilde{\rho}(\mathbf{x}_1, \mathbf{x}_2)$. If the random field is homogenous (or stationary for one-dimensional case), its covariance (and correlation) function only depends on the relative position of the pints $\mathbf{x}$ and $\mathbf{x}'$. This paper only studies the homogenous Gaussian field. The typical square exponential correlation function is given as the Eq. (16), more correlation functions can be found in [31].

$$\widetilde{\rho}\left(\mathbf{x}, \mathbf{x}'\right) = \exp\left(-\left\|\mathbf{x} - \mathbf{x}'\right\|^2 / a^2\right) \tag{16}$$

where a is the correlation length, which has large influence on the discretization of the random field.

Based on the definition, the continuous random field is defined as an uncountable indexed set of random variables, which are not convenient to implement in the numerical computation, so it needs to be discretized to countable random variables. Using the EOLE method [33] to discretize the random field, the continuous random field can be approximately expressed by

$$Y(\mathbf{x}, \theta) \approx \widehat{Y}(\mathbf{x}, \theta) = \mu + \sigma \sum_{i=1}^{m} \frac{E_i(\theta)}{\sqrt{\lambda_i}} \widetilde{\rho}_{\mathbf{xX}}^{\text{T}} \phi_i \tag{17}$$

Here μ and σ are the mean and standard deviation of the random field, $\{E_i(\theta)\}$ ($i=1,...,\ m$) denotes a set of independent standard Gaussian random variables (i.e. $E_i(\theta) \sim N(0,1)$), $\boldsymbol{\rho}_{\mathbf{xX}}$ is the correlation function vector at given nodes $\mathbf{x}_1,...,\ \mathbf{x}_q$ ($q > m$), i.e. $\widetilde{\boldsymbol{\rho}}_{\mathbf{xX}} = \left[\widetilde{\rho}\left(\mathbf{x}, \mathbf{x}_1\right), ..., \widetilde{\rho}\left(\mathbf{x}, \mathbf{x}_q\right)\right]^{\text{T}}$, λ_i are the m largest eigenvalues of the covariance matrix $\mathbf{C}_{\mathbf{XX}}$ at the given nodes, with entry $\mathbf{C}_{\mathbf{XX}}(k, l) = C\left(\mathbf{x}_k, \mathbf{x}_l\right)$, and ϕ_i are the corresponding eigenvectors.

The variance of the error for EOLE is given as

$$\text{Var}\left[Y\left(\mathbf{x}, \theta\right) - \widehat{Y}\left(\mathbf{x}, \theta\right)\right] = \sigma^2 - \sum_{i=1}^{m} \frac{1}{\lambda_i}\left(\widetilde{\boldsymbol{\rho}}_{\mathbf{xX}}^{\text{T}} \phi_i\right)^2 \tag{18}$$

The value of m can be determined by make the relative variance error be lower than a small constant, e.g. 5% used in this study. Generally, the shorter correlation length of the random field is, the more terms need to be remained. To this step, the original random field has been approximated by a series governed by the m independent standard Gaussian random variables $\{E_i(\theta)\}$.

Considering the Young's modulus and Poisson's ratio as random field and using the EOLE method to discretize them, if their correlation functions, mean and standard deviation are given, the two parameters will be re-expressed as

$$G(\mathbf{x}, \theta) = \mu_G + \sigma_G \sum_{i=1}^{m} \frac{E_i(\theta)}{\sqrt{\lambda_i}} \widetilde{\boldsymbol{\rho}}_{\mathbf{xX}}^{\text{T}} \phi_i, \kappa(\mathbf{x}, \theta) = \mu_\kappa + \sigma_\kappa \sum_{i=1}^{m} \frac{E_i(\theta)}{\sqrt{\lambda_i}} \widetilde{\boldsymbol{\rho}}_{\mathbf{xX}}^{\text{T}} \phi_i \tag{19}$$

From Eqs. (7)–(10), it can be found that the system elastic forces depend on the Young's modulus and Poisson's ratio, so it will be expressed by a function of the m random variables $E_i(\theta)$

$$\mathbf{F}(\mathbf{q}) = \mathbf{F}\left(\mathbf{q}, E_1, ..., E_m\right) \tag{20}$$

Integrating the k random variables of the rigid bodies with the m random variables of the flexible bodies, we can use one random vector to denote them, i.e. $\mathbf{E}=[E_1,...,\ E_{k+m}]^{\text{T}}$, in which the first k random variables satisfy the standard uniform distribution while the last m random variables satisfy the standard Gaussian distribution. Substituting the Eq. (14) and Eq. (20) into the Eq. (5), the dynamic equations of the rigid-flexible multibody systems with random parameters will be finally expressed by

$$\begin{cases} \mathbf{M}\left(\mathbf{E}\right)\ddot{\mathbf{q}} + \mathbf{\Phi}_{\mathbf{q}}^{\mathrm{T}}\boldsymbol{\lambda} + \mathbf{F}\left(\mathbf{q},\mathbf{E}\right) = \mathbf{Q}\left(\mathbf{q},\mathbf{E}\right) \\ \mathbf{\Phi}\left(\mathbf{q},\mathbf{E},t\right) = \mathbf{0} \end{cases} \tag{21}$$

The above DAEs contain the random variables, so it is hard to use the generalized-**α** algorithm shown in Section 2.2 to solve directly. The solving strategy of this system will be proposed in next section.

4 Methods for solving the DAEs with random variables

When the random variables are contained in the dynamic equations, the algebraic equations after discretization (Eq. 11) will be changed as the following algebraic equations

$$\mathbf{G}\left(\mathbf{q}_{i+1},\boldsymbol{\lambda}_{i+1},\mathbf{E}\right) = \begin{bmatrix} \mathbf{M}\left(\mathbf{E}\right)\ddot{\mathbf{q}}_{i+1} + \mathbf{\Phi}_{\mathbf{q}}^{\mathrm{T}}\boldsymbol{\lambda}_{i+1} + \mathbf{F}\left(\mathbf{q}_{i+1},\mathbf{E}\right) - \mathbf{Q}\left(\mathbf{q}_{i+1},\mathbf{E}\right) \\ \mathbf{\Phi}\left(\mathbf{q}_{i+1},\mathbf{E},t_{i+1}\right) \end{bmatrix} = \mathbf{0} \tag{22}$$

The aim for solving the above equation is to compute the $\mathbf{q}_{i+1}$ and $\boldsymbol{\lambda}_{i+1}$. Introducing the symbol $\mathbf{f}$ to denote the solution, i.e. $\mathbf{f} = \begin{bmatrix} \mathbf{q}_{i+1}^{\mathrm{T}} \boldsymbol{\lambda}_{i+1}^{\mathrm{T}} \end{bmatrix}^{\mathrm{T}}$, we have the following expression

$$\mathbf{f} = \left\{ \begin{bmatrix} \mathbf{q}_{i+1} \\ \boldsymbol{\lambda}_{i+1} \end{bmatrix} \middle| \mathbf{G}\left(\mathbf{q}_{i+1},\boldsymbol{\lambda}_{i+1},\mathbf{E}\right) = \mathbf{0} \right\} \tag{23}$$

As a result, the solution can be thought as a function with respect the random variables, denoted by $\mathbf{f}(\mathbf{E})$. It should be noted that the analytical expression of this function is not known, so the function value can only be obtained by using the numerical method, i.e. solving the Eq. (22) by fixing the random variables at given values. Since the random variables satisfy some probability distribution, the function value should also have the statistical characteristics. The main work is how to get their statistical characteristics, including the mean and variance.

4.1 Statistical methods

The most direct method is to use the Monte Carlo method to obtain the statistical information of the response. Use the random sampling method to produce a large number of sampling points of the random variables, and then solve the Eq. (22) by fixing the random variables at these sampling points, which will produce a large number of samples of the solution. The unbiased estimation of the mean and variance of the response can be obtained by

$$\boldsymbol{\mu}_{\mathbf{f}} = \frac{1}{N}\sum_{i=1}^{N}\mathbf{f}\left(\tilde{\mathbf{E}}_i\right), \quad \sigma_{\mathbf{f}}^2 = \frac{1}{N-1}\sum_{i=1}^{N}\left(\mathbf{f}\left(\tilde{\mathbf{E}}_i\right) - \boldsymbol{\mu}_{\mathbf{f}}\right)^2 \tag{24}$$

where N is the number of samples, and $\tilde{\mathbf{E}}_i$ are the sampling points of random variables. One important advantage of the Monte Carlo method is that it has no limitation for the format of function $\mathbf{f}(\mathbf{E})$, which means that $\mathbf{f}(\mathbf{E})$ can be smooth or non-smooth, or even discontinuous. Another advantage is that the Monte Carlo method does not have dimensional curse problem because its accuracy only depends on the sampling size. Therefore, it is quite appropriate for high dimensional problems. Based on the large number theorem, the convergence ratio of Monte Carlo method is proportion to $1/\sqrt{N}$, so it requires a large number of sampling points to get an acceptable accuracy. In this study, solving the Eq. (22) is usually time-consuming, so we cannot use too many sampling points. As a result, the Monte Carlo method is only used to produce the reference solution.

To improve the efficiency of Monte Carlo method, an approach is to use a more efficient sampling method to select the sampling points. The Latin Hypercube sampling (LHS) method [57–59] shows quite good performance in statistics, so it will be employed to produce the sampling points. After the sampling points are produced, we can repeat the same procedure of the general Monte Carlo method, and then the mean and variance of response can be obtained, termed as LHS-based statistical method. The convergence ratio of LHS-based statistical method is much higher than the general Monte Carlo method, which will be shown in Section 5.

4.2 Polynomial Chaos expansion method

The basic idea of PC expansion is to use a polynomials function $\mathbf{f}_n(\mathbf{E}) \in P_n(\mathbf{E})$ to approximate the original function $\mathbf{f}(\mathbf{E})$, where the $P_n(\mathbf{E})$ is the space of polynomials of random variable $\mathbf{E}$ of order up to $n \geq 0$. After the approximated polynomials function is obtained, the mean and variance of the original function $\mathbf{f}(\mathbf{E})$ will be estimated by using the $\mathbf{f}_n(\mathbf{E})$.

Considering the 1-dimensional random variable first, for any function $\mathbf{f}(E)$ in the mean-square integrable space, its nth-degree PC expansion is defined as

$$\mathbf{f}\left(E\right) \approx \mathbf{f}_n\left(E\right) = \sum_{i=0}^{n}\hat{\mathbf{f}}_i\Psi_i\left(E\right), \quad \hat{\mathbf{f}}_i = \frac{1}{\gamma_i}E\left[\mathbf{f}\left(E\right)\Psi_i\left(E\right)\right] \tag{25}$$

Here E[g] represents the expectation or mean of g. In the approximation theory, $\mathbf{f}_n(E)$ is the best approximation of $\mathbf{f}(E)$ in the least-square sense if $\mathbf{f}(E) \in C[a, b]$, such that

$$\left\| \mathbf{f}\left(E\right) - \mathbf{f}_n\left(E\right) \right\|^2 = \inf_{\mathbf{p}_n \in P_n}\left\| \mathbf{f}\left(E\right) - \mathbf{p}_n\left(E\right) \right\|^2 = \inf_{\mathbf{p}_n \in P_n}\int_a^b \bar{\rho}\left(E\right)\left[\mathbf{f}\left(E\right) - \mathbf{p}_n\left(E\right)\right]^2 dE \tag{26}$$

where the $\bar{\rho}$ denotes the weight function, which is the probability density function of the random variable E. Therefore, the Eq. (25) gives the minimum mean-square error under the given weight for the nth-degree polynomial approximation.

The $\hat{\mathbf{f}}_i$ in Eq. (25) is the coefficients of the PC expansion, and $\Psi_i(E)$ denotes PC basic functions that are the orthogonal polynomial functions satisfying the following equation.

$$E\left[\Psi_i(E)\Psi_j(E)\right] = \gamma_i\delta_{ij}, \ \ \gamma_i = E\left[\Psi_i^2(E)\right], \ \ i,j = 0,1,...,n \qquad \textbf{(27)}$$

where γ_i are the normalization factors, and δ_{ij} is the Kronecker delta function. For the continuous random variable E, the orthogonality can be expressed by

$$E\left[\Psi_i(E)\Psi_j(E)\right] = \int \bar{\rho}(\varepsilon)\Psi_i(\varepsilon)\Psi_j(\varepsilon)\,d\varepsilon = \gamma_i\delta_{ij} \qquad \textbf{(28)}$$

Therefore, the $\{\Psi_i(\varepsilon)\}$ are orthogonal polynomials of $\varepsilon\in R$ with the weight function $\bar{\rho}(\varepsilon)$, which is also the probability density function of the random variable E. By using the orthogonality of the basic functions, the coefficients can be computed by the following formula

$$\hat{\mathbf{f}}_i = \frac{1}{\gamma_i}E\left[\mathbf{f}(E)\Psi_i(E)\right] = \frac{1}{\gamma_i}\int \bar{\rho}(\varepsilon)\mathbf{f}(\varepsilon)\Psi_i(\varepsilon)\,d\varepsilon \qquad \textbf{(29)}$$

For the standard Gaussian random variable, i.e. $E\sim N(0,1)$, its probability density function is given as $\bar{\rho}(\varepsilon) = e^{-\varepsilon^2/2}/\sqrt{2\pi}$, and the corresponding orthogonal polynomials are the Hermite polynomials. For the standard uniform random variable $E\sim U(-1,1)$, its probability density function is $\bar{\rho}(\varepsilon) = 1/2$, and the corresponding orthogonal polynomials are the Legendre polynomials.

Since the PC basic functions have been known, the key of PC expansion is to compute the coefficients. When the Eq. (29) is used to compute the coefficients, the numerical quadrature method has to be employed, because the analytical expression of function $\mathbf{f}$ is not known. By employing the Kth-order Gaussian quadrature formula [60], the coefficients can be computed by

$$\hat{\mathbf{f}}_i = \frac{1}{\gamma_i}\int \bar{\rho}(\varepsilon)\mathbf{f}(\varepsilon)\Psi_i(\varepsilon)\,d\varepsilon \approx \sum_{j=1}^{K}\frac{1}{\gamma_i}w_j\mathbf{f}\left(\varepsilon_j\right)\Psi_i\left(\varepsilon_j\right) \qquad \textbf{(30)}$$

where w_j is the integral coefficient, and ε_j denotes the interpolation points that are the roots of Kth-order orthogonal polynomial $\Psi_K(\varepsilon)$. The algebraic precision order of this quadrature formula is be $2K-1$. Using higher order interpolation points gives higher integral accuracy, but it increases the computational cost, because each one interpolation point added means one more call of solving the rigid-flexible multibody systems. To trade-off the efficiency and accuracy, the order of this formula is usually set as $K=n+1$.

For the multi-dimensional case, such as the $k+m$ dimensional random variables in Section 3.2, the bases are defined as the product of the each univariate orthogonal polynomials, i.e.

$$\Psi_{\mathbf{i}}(\mathbf{E}) = \prod_{j=1}^{k+m}\Psi_{i_j}\left(E_j\right), \ \ i_j = 0,1,... \qquad \textbf{(31)}$$

where the subscript $\mathbf{i}$ is a $(k+m)$-dimensional multi-index. As a result, the nth-order PC expansion of function $\mathbf{f}(\mathbf{E})$, $\mathbf{E}\in R^{k+m}$, is expressed as the following equation

$$\mathbf{f}(\mathbf{E}) = \mathbf{f}_n(\mathbf{E}) \approx \sum_{|\mathbf{i}|_0\leq n}\hat{\mathbf{f}}_{\mathbf{i}}\Psi_{\mathbf{i}}(\mathbf{E}), \ \ \hat{\mathbf{f}}_{\mathbf{i}} = \frac{1}{\gamma_{\mathbf{i}}}E\left[\mathbf{f}(\mathbf{E})\Psi_{\mathbf{i}}(\mathbf{E})\right] = \frac{1}{\gamma_{\mathbf{i}}}\int \bar{\rho}(\boldsymbol{\varepsilon})\mathbf{f}(\boldsymbol{\varepsilon})\Psi_{\mathbf{i}}(\boldsymbol{\varepsilon})\,d\boldsymbol{\varepsilon} \qquad \textbf{(32)}$$

where $|\mathbf{i}|_0 = \max\ i_j, \ 1\leq j\leq k+m$, and the number of coefficients is $s=(n+1)^{k+m}$. The coefficients can still be computed by the multi-dimensional Gaussian integral formula or by the least square method [44], and the interpolation points will be the tensor product of the roots of univariate orthogonal polynomials with order $n+1$ in $k+m$ dimensional space, expressed as

$$\tilde{\boldsymbol{\varepsilon}} = \boldsymbol{\varepsilon}_1\otimes\cdots\otimes\boldsymbol{\varepsilon}_{k+m}, \ \ \boldsymbol{\varepsilon}_i = \left[\varepsilon_{i,1},\cdots\varepsilon_{i,n+1}\right]^{\mathrm{T}}, \ \ i = 1,2,...,k+m \qquad \textbf{(33)}$$

It should be noted that the number of interpolation points equals to the number of coefficients in PC expansion, i.e. $(n+1)^{k+m}$, which increases exponentially with the increase of dimension. Figs. 3 and 4 show the interpolation points in 2-dimensional space of uniform random variables and Gaussian random variables with order 5, respectively.
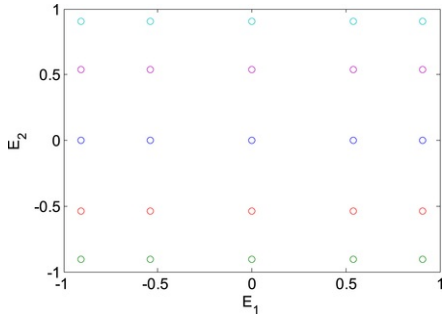
Fig. 3 The interpolation points for $\mathbf{E} \sim U(-1,1)^2$.

alt-text: Fig. 3

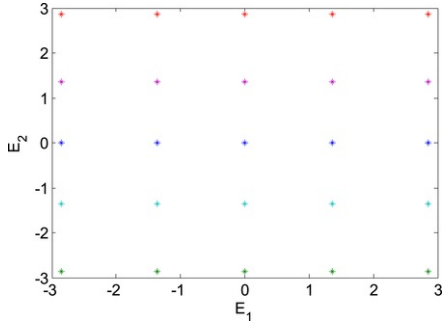**Fig. 4** The interpolation points for $\mathbf{E} \sim N(0,1)^2$.

alt-text: Fig. 4

After the PC expansion is finished, the statistical methods can be employed to get its mean and variance. This process does not increase the computation burden much, because the analytical expression of the functions has been obtained. However, there is another more convenient way to compute the mean and variance. By using the orthogonality of the PC basic function, the mean and variance can be computed by

$$\boldsymbol{\mu}_{\mathbf{f}} = E\left[\mathbf{f}\left(\mathbf{E}\right)\right] \approx \int \sum_{|\mathbf{i}|_0 \leq n} \widehat{\mathbf{f}}_{\mathbf{i}} \Psi_{\mathbf{i}}\left(\varepsilon\right) d\varepsilon = \widehat{\mathbf{f}}_{\mathbf{0}}, \quad \boldsymbol{\sigma}_{\mathbf{f}}^2 = E\left[\left(\mathbf{f}\left(\mathbf{E}\right) - \boldsymbol{\mu}_{\mathbf{f}}\right)^2\right] \approx \sum_{0 < |\mathbf{i}|_0 \leq n} \gamma_{\mathbf{i}} \widehat{\mathbf{f}}_{\mathbf{i}}^2 \qquad \textbf{(34)}$$

The error of the mean is only induced by the numerical integral error from Eq. (30), while the error of variance is induced by two parts, which are the truncated error in Eq. (25) and the numerical integral error from Eq. (30). As a result, the mean usually has higher accuracy than the variance. Specifically, in Eq. (30), the error will be quite large if the function $\mathbf{f(E)}$ is unsmooth (or contains many high frequency signals), which does not often occur in traditional mechanics problem of structures but is quite common for the rigid-flexible multibody systems studied in this paper. More detailed analysis about the error will be provided in Section 5.

4.3 Numerical implementation process

The numerical implementation process can be illustrated by the flowchart Fig. 5, which mainly contains 4 steps: (1) determine the uniform random variables of the geometry size and discrete the random field of material properties to a finite standard Gaussian random variables; (2) produce the sampling points by using the LHS and the interpolation points of PC expansion; (3) build the dynamic equations of rigid-flexible multibody systems using the ANCF-based method, and then solve the equations using general-$\boldsymbol{\alpha}$ method by fixing the values of random variables to be the sampling points and interpolation points; (4) compute the mean and variance by using the statistical method and PC expansion method.
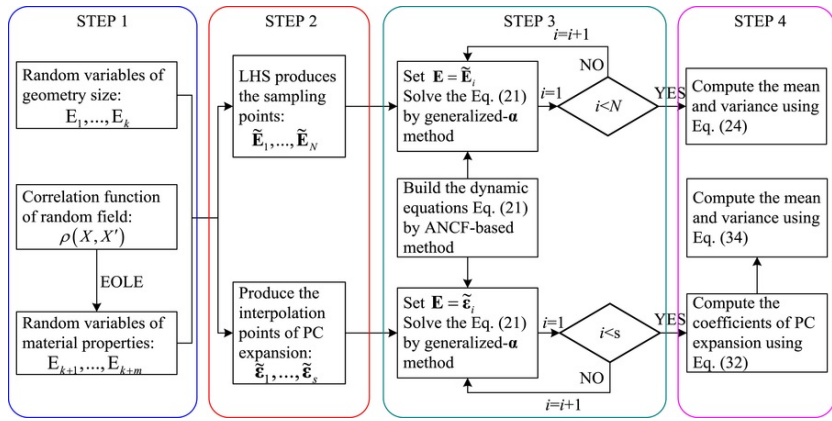
Fig. 5 Flowchart of solving rigid-flexible multibody system with random parameters.

alt-text: Fig. 5

5 Application on the slider crank mechanism

In this section, a slider-crank mechanism is used as the numerical examples to show the accuracy and stability of the proposed uncertain analysis method.

The schematic of slider-crank mechanism is shown in Fig. 6, in which the slider and crank are considered as rigid body, while the link is made by aluminum that is thought as flexible body. Three ANCF elements are used to build the model of flexible link, where the nodes are denoted by points A, D, E, and B. The rotation velocity of the crank is $\omega=2\pi$ rad/s, and the deformation of the spring is zero in the position shown in the figure. The geometry of all components is prismatic, and some parameters under the deterministic case are provided in Table 1. As the crank and slider are considered to be rigid bodies, there is no elastic force produced by the bodies, so the Young's modulus and Poisson's ratio are not provided in Table 1.
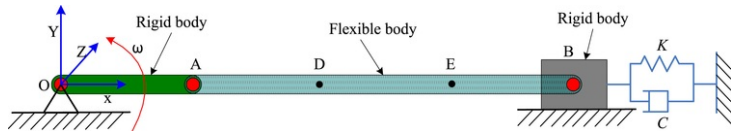
Fig. 6 The schematic of slider-crank mechanism.

alt-text: Fig. 6

Table 1 The parameters of the slider-crank mechanism.

alt-text: Table 1

Component	Density (kg/m³)	Length/X (m)	Height/Y (m)	Width/Z (m)	Young's modulus (GPa)	Poisson's ratio
Crank	7800	0.2	0.01	0.01	–	–
Link	2700	0.6	0.01	0.01	69	0.34
Slider	7800	0.08	0.08	0.2	–	–

5.1 Long correlation length of random field

Assume that the length of the crank satisfies the uniform distribution $l\sim U(0.19, 0.21)$, which can be expressed by the standard uniform random variable, i.e. $l=0.2+0.01E_1$, where $E_1\sim U(-1, 1)$. At the same time, the Young's modulus of the link is considered as a homogenous Gaussian field with 2 m correlation length in X direction, so the correlation function is given as

$$\rho\left(X, X'\right) = \exp\left(-\left\|X - X'\right\|^2/2^2\right) \tag{35}$$

The mean of the Young's modulus is the value shown in Table 1, and the standard deviation is 1% of mean, i.e. 0.69 GPa. Use the EOLE method to discretize the random field, truncated by 1 term, which means the random field is discretized to one Gaussian random variable.

The error of variance after the discretization is shown in Fig. 7, which indicates that the maximum error is about 0.043<5% required by this study. As a result, there are two random variables in this system, which are the $E_1 \sim U(-1, 1)$ and $E_2 \sim N(0, 1)$. The stiffness of the spring and damping ratio are considered in two cases, which are (1) K=1000 N/m, C=100 Ns/m; (2) K=10 N/m, C=1 Ns/m.

(1) K=1000 N/m, C=100 Ns/m
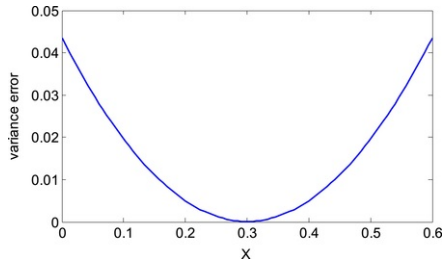
Fig. 7 The discretization error of random field with 2 m correlation length.

alt-text: Fig. 7

If the second order PC expansion is used to approximate the uncertain solution, there will be 3^2=9 interpolation points, shown as Fig. 8(a). The LHS is used to produce the same number of sampling points, which are shown in Fig. 8(b). Based on the 9 interpolation points and 9 sampling points, implementing the third step and fourth step shown in Fig. 5 gets the mean and standard deviation of the system responses. The following four responses are considered as evaluation indexes: 1) q_X: the displacement of the node B in X direction, 2) q_Y: displacement of the node E in Y direction, 3) F_X: the reaction force at point A in X direction, 4) F_Y: the reaction force at point A in X direction.
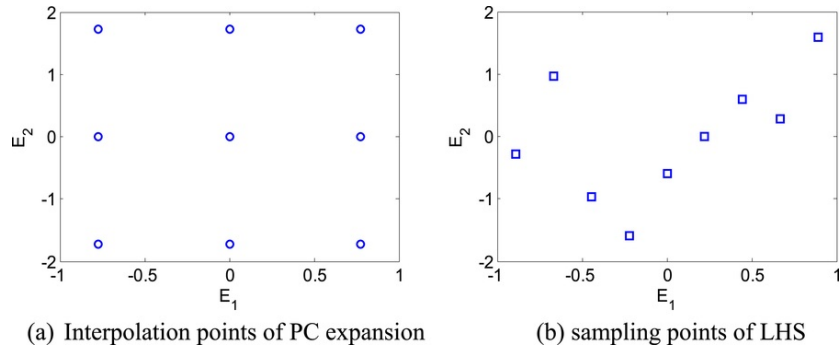
(a) Interpolation points of PC expansion   (b) sampling points of LHS

Fig. 8 Distribution of interpolation points and sampling point. (a) Interpolation points of PC expansion (b) sampling points of LHS.

alt-text: Fig. 8

To validate the results, the general Monte Carlo method with 1000 random samples is used as the reference. Fig. 9 shows the mean responses, where the legend 'PC', 'LHS', and 'MC' denote the results obtained by PC expansion method, LHS-based statistical method, and general Monte Carlo method, respectively. It can be found that the three curves are coincidence, which indicates both the PC expansion and LHS-based statistical methods can catch the mean responses only with 9 simulations. Compared to the 1000 simulations used in the Monte Carlo method, the efficiency of the PC expansion and LHS-based statistical methods are higher.
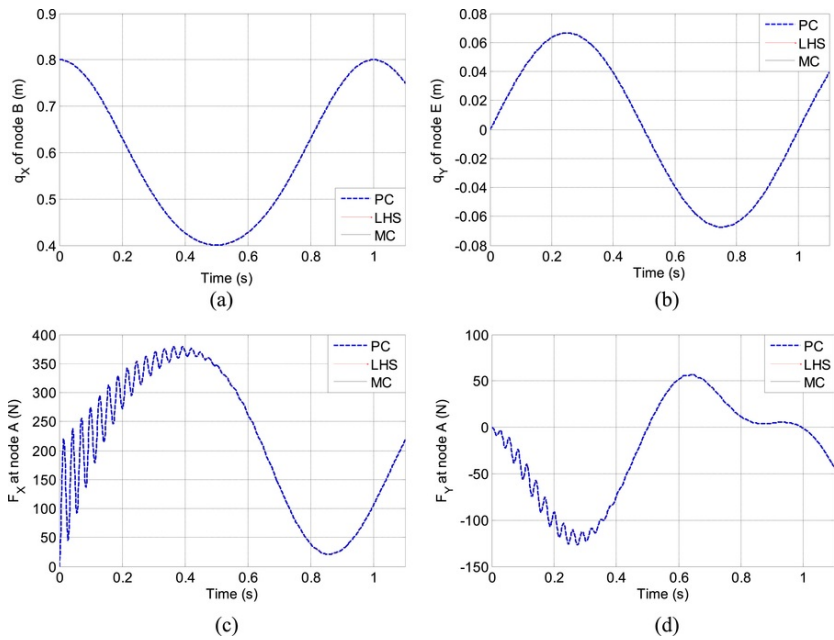
Fig. 9 Mean responses by using 9 samples (high stiffness and damping ratio).

alt-text: Fig. 9

For the standard deviation shown in Fig. 10, the PC expansion method still gives quite close results to the Monte Carlo method, while the LHS-based statistical method shows larger difference, especially for the two reaction forces. The 9 samples for LHS-based statistical method are not enough to get a good estimation of the standard deviation.
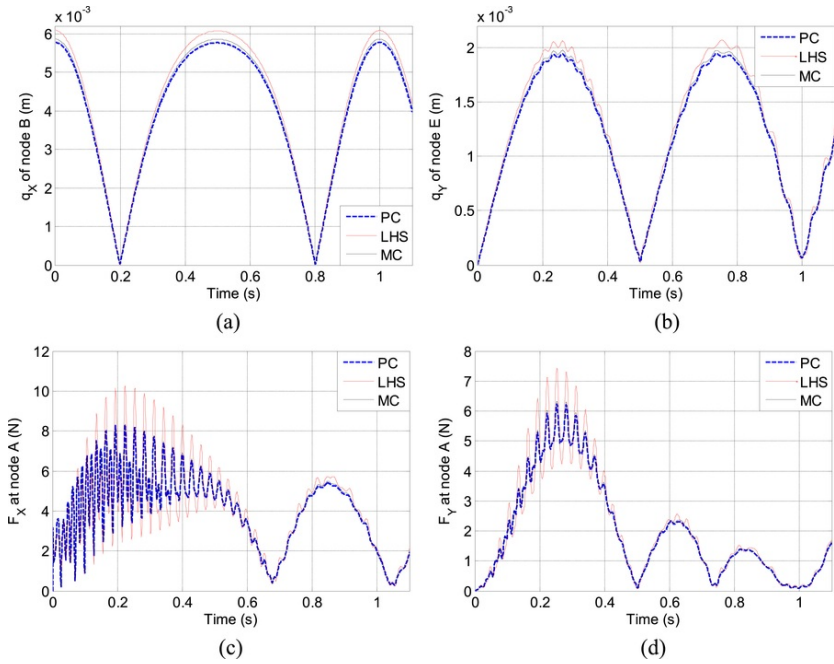
Fig. 10 Standard deviations by using 9 samples (high stiffness and damping ratio).

alt-text: Fig. 10

To describe the accuracy of the proposed method more clearly, define the error of the mean and standard deviation of the proposed method as follows

$$
e_\mu = \frac{\int_0^{t_{end}} |\hat{\mu} - \tilde{\mu}| \, dt}{\int_0^{t_{end}} |\tilde{\mu}| \, dt}, \quad e_\sigma = \frac{\int_0^{t_{end}} |\hat{\sigma} - \tilde{\sigma}| \, dt}{\int_0^{t_{end}} |\tilde{\sigma}| \, dt} \tag{36}
$$

where $\hat{\mu}$ and $\hat{\sigma}$ are the mean and standard deviation obtained by the PC expansion or LHS-based statistical method, $\tilde{\mu}$ and $\tilde{\sigma}$ denote the mean and standard deviation obtained by the Monte Carlo method, t is the time. It should be noted that the error defined in Eq. (36) is the difference between the PC expansion (or LHS-based statistical) method and the general Monte Carlo method with 1000 samples. Since the Monte Carlo method also contains some minor errors, this difference may not be quite accurate when it is extremely small, but it can conclude that a method is bad if this difference is too large.

To compare the accuracy of the PC expansion and LHS-based statistical methods under different sampling size, the order of PC expansion is set as 2, 4, 6, and 8, respectively, so the corresponding sampling size will be 9, 25, 49, and 81, respectively. The error of the mean and standard deviation changing with the sampling size are shown in Figs. 11 and 12. The error of mean is quite small (almost smaller than 0.001), so it does not change much with the increase of sampling size. When the order of PC expansion increases, the mean does not change, which indicates that the second order Gaussian quadrature formula is accurate for computing the first coefficient (Eq. (31)). The fluctuation of the LHS-based statistical method is induced by the randomness of the sampling points, because there are some random factors in producing the sampling points by the LHS-based statistical method. The error of standard deviation obtained by the PC expansion method is still quite stable, almost keeping the same with the sampling size increasing, which demonstrates that the high-order coefficients of PC expansion is quite small compared to its low-order coefficients. However, the fluctuation of the LHS-based statistical method is obvious, and its error gets closer to that of PC expansion method when the sampling size increases. In summary, the PC expansion method can provide higher accuracy and more stable results than the LHS-based statistical method in the case of high spring stiffness and damping ratio.
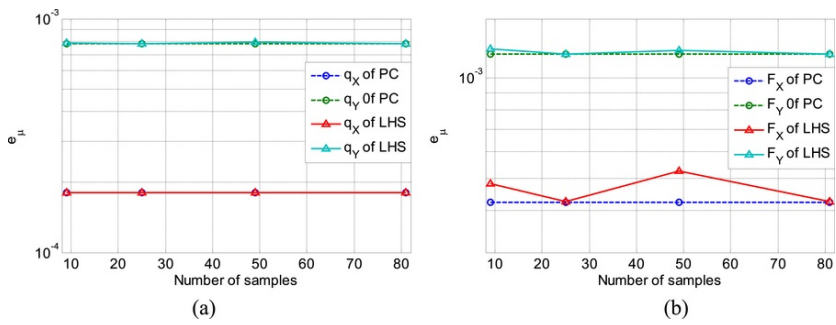
(2) K=10 N/m, C=1 Ns/m

Fig. 11 The error of mean responses changing with sampling size.
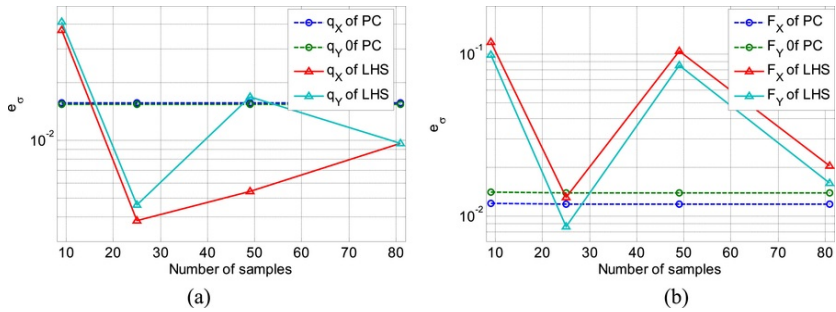
alt-text: Fig. 11

Fig. 12 The error of standard deviations changing with sampling size.

alt-text: Fig. 12

When the spring stiffness and damping ratio are decreased, the responses of the mechanism will change. Fig. 13 shows the configuration of the slider-crank mechanism, where the label 'HIGH' denotes the high stiffness and damping ratio while the label 'LOW' denotes the low stiffness and damping ratio. It can be found that the deformation of the link under the two cases is obviously different.
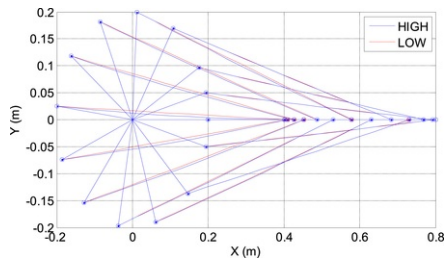
Fig. 13 The configuration of the slider-crank mechanism.

alt-text: Fig. 13

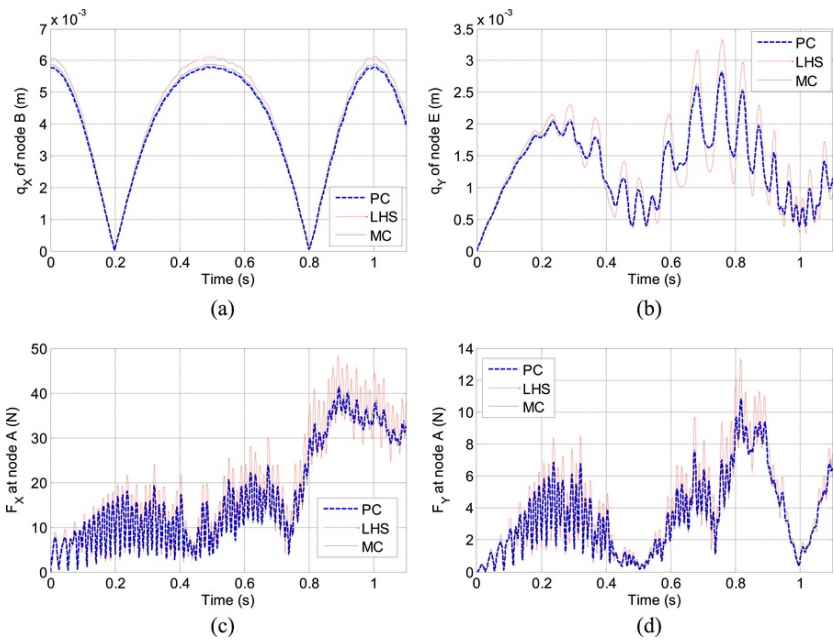The mean responses with 9 sampling points are shown in Fig. 14.
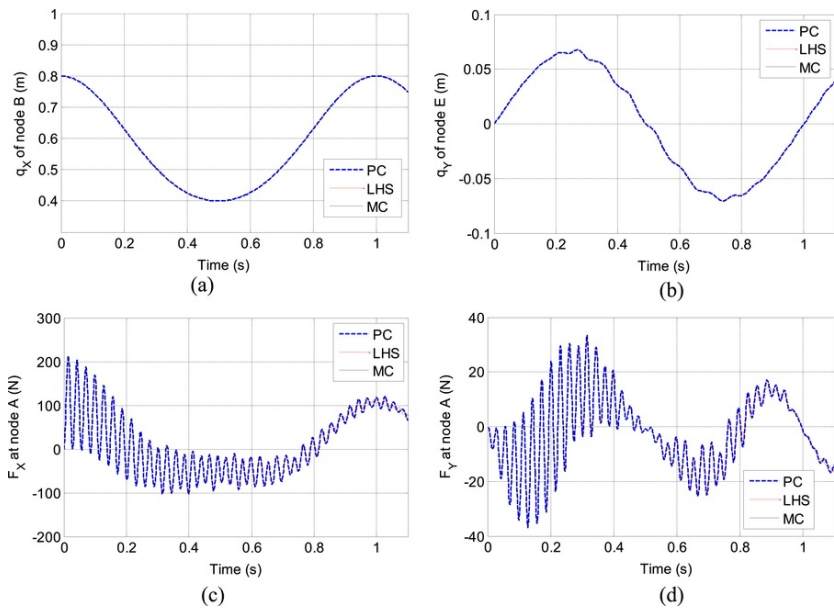
Fig. 14 Mean responses by using 9 samples (low stiffness and damping ratio).

alt-text: Fig. 14

Compared to the high stiffness and damping case, there are some fluctuations in the response of q_Y and the reduction of the fluctuation of F_X and F_Y become slowly, because the damping ratio is much lower. For the displacements, the PC expansion and LHS-based statistical methods give almost the same results as the Monte Carlo method, so both have high accuracy. However, for the reaction forces, the LHS-based statistical method shows difference, while the PC expansion method gives a quite coincident result to the Monte Carlo method.

The standard deviations by using 9 sampling points are shown in Fig. 15. The displacement of q_X does not show much difference compared to the high spring stiffness and damping case and the PC expansion method is closer to the Monte Carlo method than the LHS-based statistical method. There are more high frequency signals for other three responses, and the magnitude of the fluctuation of the LHS-based statistical method is much larger than the Monte Carlo method while the PC expansion method shows quite similar solution to the Monte Carlo method. Hence, the PC expansion method has better performance than the LHS-based statistical method when a small number of sampling points (or interpolation points) are used.

Fig. 15 Standard deviations by using 9 samples (low stiffness and damping ratio).

alt-text: Fig. 15

Similar to the high stiffness and damping case, the PC expansion and LHS-based statistical methods with different number of sampling points are investigated, shown in Figs. 16 and 17. The mean responses of the PC expansion method are more accurate and stable than the LHS-based statistical methods. The randomness of the samples makes the LHS-based statistical method have a fluctuated performance.
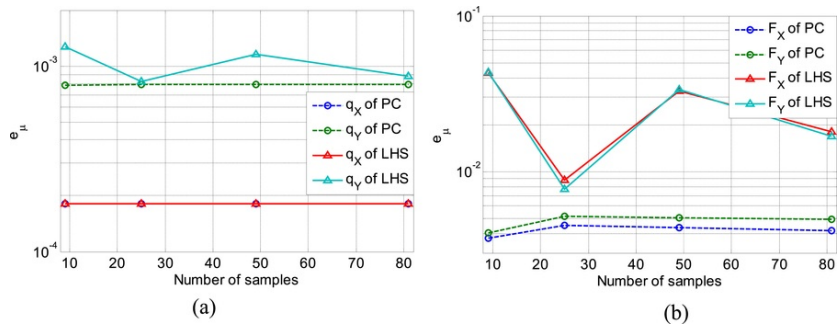

Fig. 16 The error of mean responses changing with sampling size.

alt-text: Fig. 16
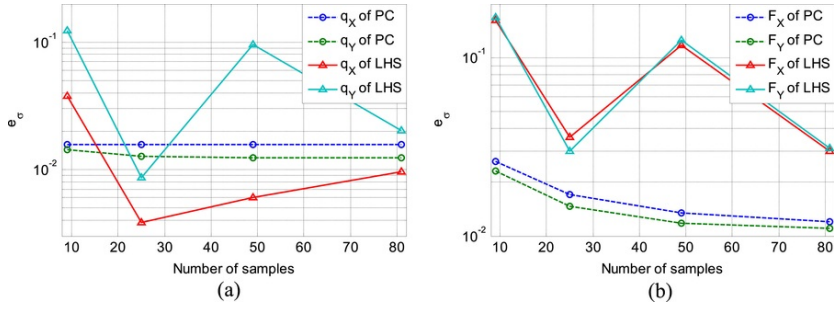
Fig. 17 The error of standard deviations changing with sampling size.

alt-text: Fig. 17

As stated in Section 4, the error of the standard deviations is usually larger than the error of mean, which can be found from Fig. 17. Except the q_X, all other three responses indicate the PC expansion method has higher accuracy for the standard deviations. With the increase of sampling size, the error of the q_Y, F_X, and F_Y of the PC expansion method decreases sequentially, this demonstrates that the high-order coefficients of the PC expansion are large in this case. The LHS-based statistical method still shows unstable results for the standard deviations. In summary, when the correlation length of the random field is relatively long (2 m in this example), the PC expansion method shows better performance than the LHS-based statistical method for both the accuracy and stability.

5.2 Short correlation length of random field

In this subsection, the geometry uncertainty of the crank is considered to be the same as the last subsection, i.e. $l \sim U(0.19, 0.21)$, but the Poisson's ratio of the link will be considered as the random field with a shorter correlation length while the Young's modulus is deterministic. Assuming the correlation length is 1 m in X direction, so the correlation function is given as

$$\rho\left(X, X'\right) = \exp\left(-\left\|X - X'\right\|^2 / l^2\right) \tag{36}$$

The mean of the Poisson's ratio is 0.34, and the standard deviation is 1% of its mean value, i.e. 0.0034. The EOLE method is used to discreet the random field, truncated by two terms. The error of the discretization is shown in Fig. 18, where the maximum error (0.0062) is smaller than 5%. Therefore, after the discretization, the random field is transformed to two standard Gaussian variables, and there will be three random variables for the whole system, i.e. $E_1 \sim U(-1, 1)$, $E_2 \sim N(0, 1)$, and $E_3 \sim N(0, 1)$. Similar to last subsection, the stiffness of the spring and the damping ratio are considered to be high and low cases.
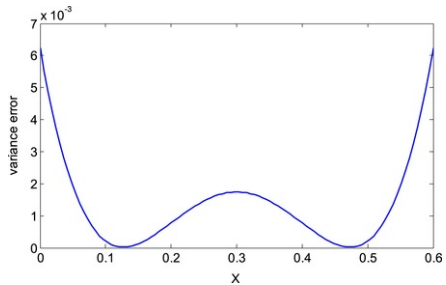
(1) K=1000 N/m, C=100 Ns/m

Fig. 18 The discretization error of 1 m correlation length.

alt-text: Fig. 18

The second order PC expansion is considered first, so there will be 3^3=27 interpolation points being used, and the LHS-based statistical method uses the same number of samples to estimate the responses.

Fig. 19 shows the mean responses of the two methods and the Monte Carlo method with 1000 random samples. For the displacements q_X and q_Y, both the PC expansion and LHS-based statistical methods provide very close

solution to the Monte Carlo method. The accuracy of reaction forces is not as good as the displacements, but it is also acceptable. It should be noted that only 27 samples are used in the PC expansion and LHS-based statistical methods, so they are much more efficient than the general Monte Carlo method that requires 1000 samples.
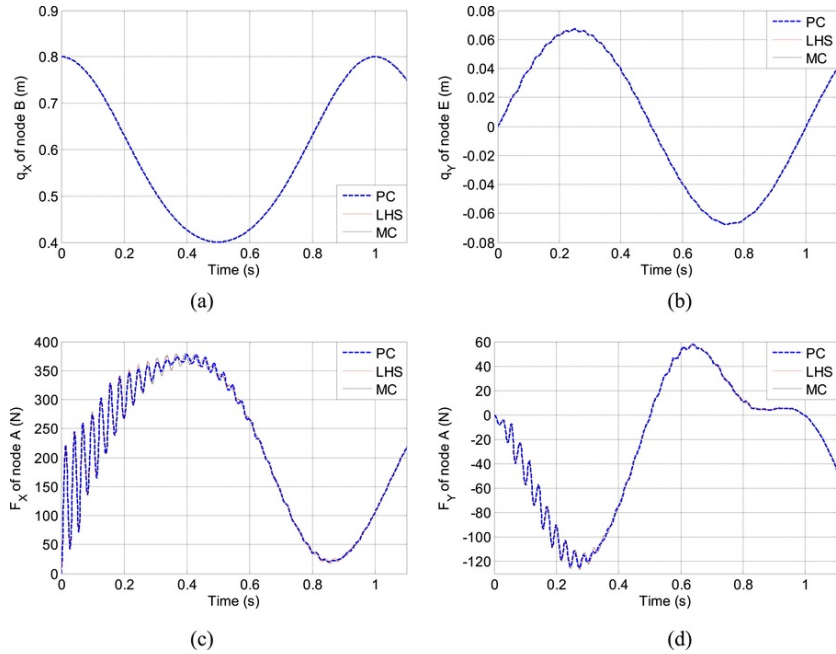

Fig. 19 Mean responses by using 27 samples (high stiffness and damping ratio).

alt-text: Fig. 19

The standard deviations are shown in Fig. 20. The PC expansion method gives a higher accuracy than the LHS-based statistical method for the displacements, but the latter is better for the reaction forces. It should be noted that the accuracy of the standard deviations is lower than the mean responses.
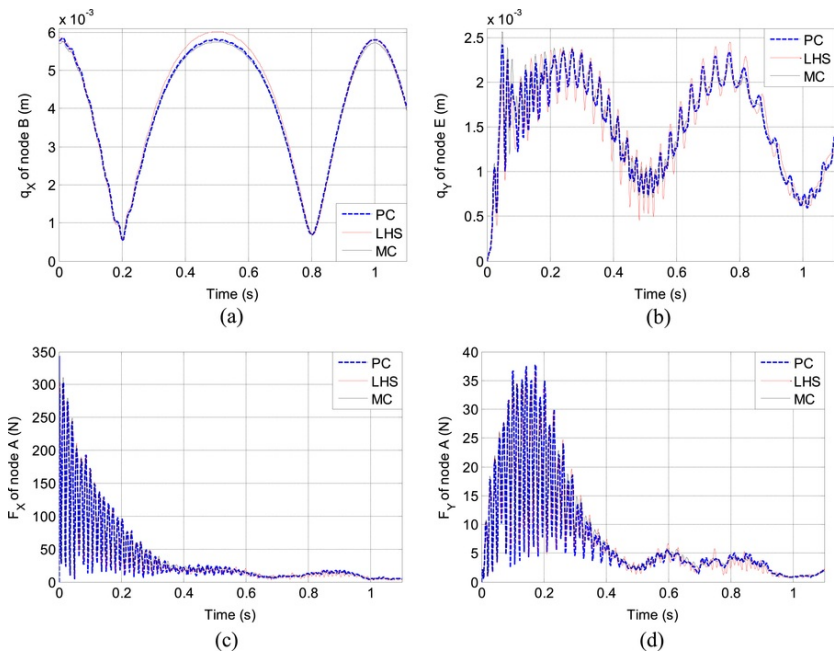
Fig. 20 Standard deviations by using 27 samples (high stiffness and damping ratio).

alt-text: Fig. 20

Considering the order of PC expansion to be 2, 3, and 4, the sampling size will be 27, 64, and 125, respectively. The accuracy of the mean responses under different sampling size is given in Fig. 21. The accuracy of the LHS-based statistical method is higher than the PC expansion method under all different sampling sizes, which is contrary to the case of long correlation length shown in Section 5.1. Especially for the reaction forces, the error of LHS-based statistical method is almost one half of the error of PC expansion method. The fluctuation of LHS-based statistical method is induced by the randomness of samples, while the fluctuation of PC expansion method is induced by the numerical error of Gaussian quadrature formula.
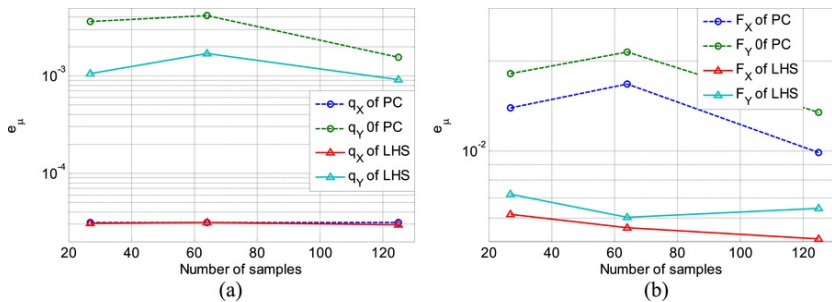
Fig. 21 The error of mean responses changing with sampling size.

alt-text: Fig. 21

The error of standard deviations is provided in Fig. 22. The q_X of PC expansion method is better than the LHS-based statistical method, but all other three responses of which have smaller error. The convergence ratio of LHS-based statistical method is higher and more stable than PC expansion method. Also, the error of standard deviations is larger than that of mean responses, which is coincident with the Figs. 19 and 20. In summary, except the response of q_X, all other three responses indicate that the LHS-based statistical method has higher accuracy and more stability than the PC expansion method.

(2) K=10 N/m, C=1 Ns/m
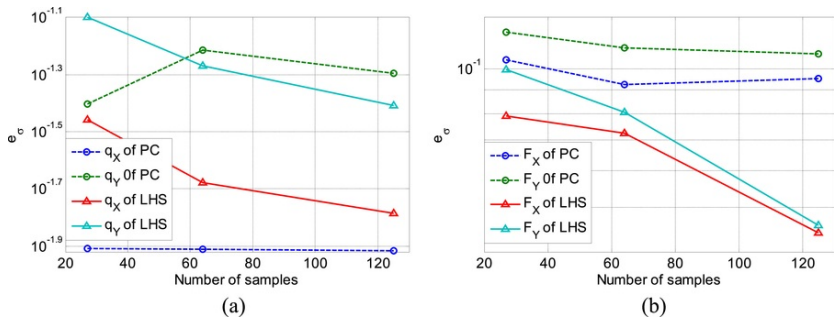

(a)   (b)

Fig. 22 The error of standard deviations changing with sampling size.

alt-text: Fig. 22

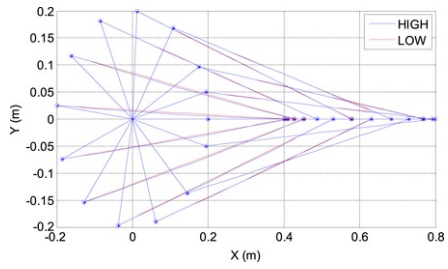The configuration of the mechanism is shown in Fig. 23.

Fig. 23 The configuration of the slider-crank mechanism.

alt-text: Fig. 23

When the spring stiffness and damping ratio decreases, the responses will contain more high-frequency signals in the time domain, which can be found in the Fig. 24. For the 27 sampling points, the mean displacements are accurate for both the PC expansion and LHS-based statistical methods, but the error of the mean reaction forces are quite large. The sampling size may be too small to get acceptable accuracy, so more sampling points should be used.
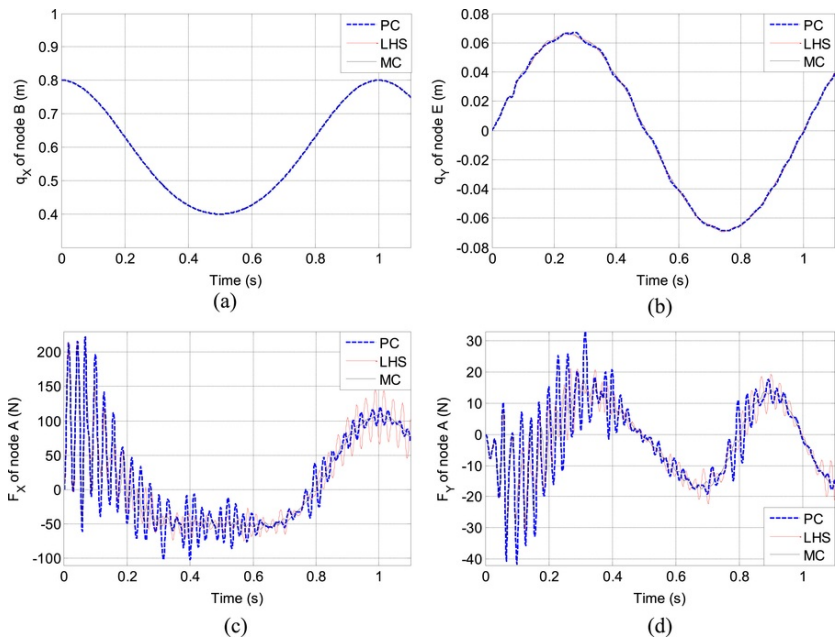
Fig. 24 Mean responses by using 27 samples (low stiffness and damping ratio).

alt-text: Fig. 24

The standard deviations under the 27 samples are shown in Fig. 25. The accuracy of the q_X is obviously better than other three responses, and the PC expansion method also shows better performance for this response. The two methods show similar accuracy for the standard deviation of the q_Y, but the LHS-based statistical method has higher accuracy in estimating the standard deviations of F_X, and F_Y. We may find that the standard deviations of the reaction forces are even larger than their mean responses. In fact, both of the two methods do not have high accuracy for estimating the standard deviation of q_Y, F_X, and F_Y, so more sampling points have to be used to get an acceptable accuracy.
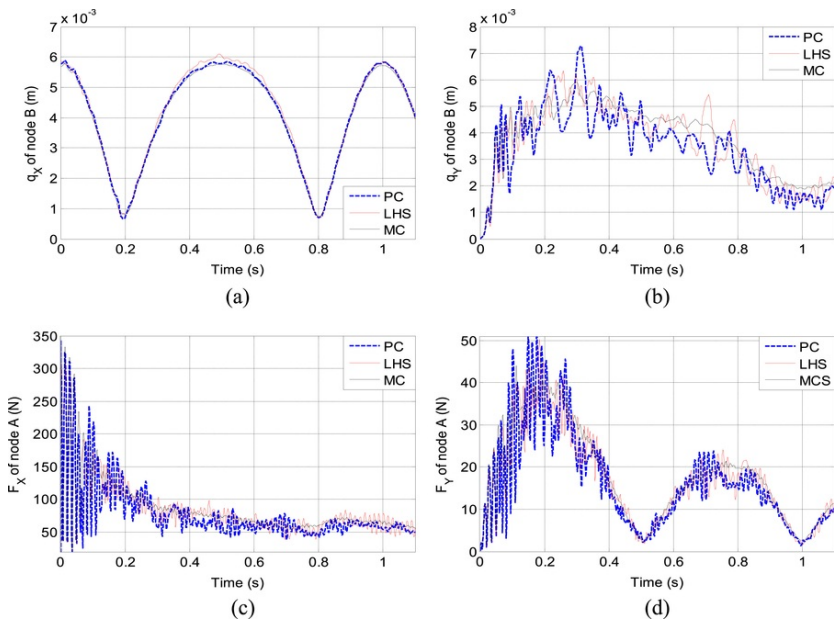
Fig. 25 Standard deviations by using 27 samples (low stiffness and damping ratio).

alt-text: Fig. 25

Fig. 26 provides the error of mean response under different sampling size. The accuracy of the mean displacements is higher than that of the reaction forces. All the four mean responses indicate the LHS-based statistical method has higher accuracy than the PC expansion method, no matter what the sampling size is. It should be noted that the error of the mean reaction forces is quite large. Even though the 125 sampling points are used, their error is still larger than 10%.
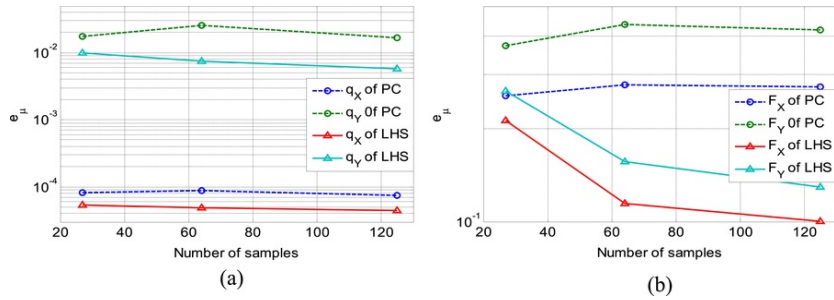

Fig. 26 The error of mean responses changing with sampling size.

alt-text: Fig. 26

The error of standard deviations under different sampling size is shown in Fig. 27, which demonstrates that the error decreases sequentially with the sampling size increasing. Similar to the previous cases, the PC expansion method has higher accuracy in estimating the standard deviation of q_X. However, the LHS-based statistical method shows better performance for other three responses, providing only less than one half of the error of the PC expansion method. Another phenomenon should be mentioned is that the error of standard deviation (Fig. 27(b)) is smaller than the error of mean responses (Fig. 26(b)) for the reaction forces. If the standard deviation is larger than its mean, estimating the standard deviation may be easier than estimating the mean.
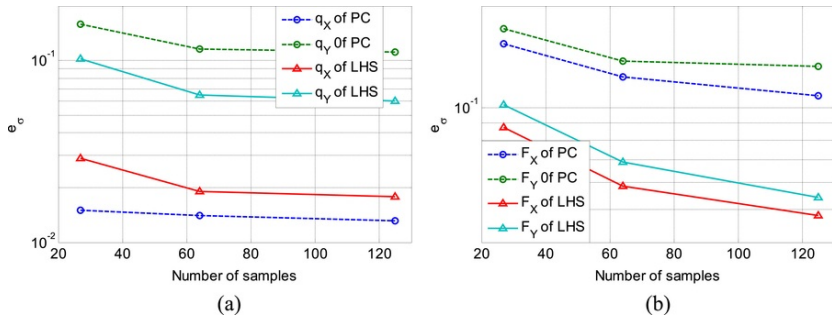
Fig. 27 The error of standard deviations changing with sampling size.

alt-text: Fig. 27

For the short correlation length of the random field, the LHS-based statistical method shows better performance than the PC expansion method in most cases, which is contrary to the case of long correlation length. Next, a more detailed discussion will be provided to express which method is better under different conditions.

5.3 Discussion of the PC expansion and LHS-based statistical methods

The highest order of the PC expansion is 4 in the last subsection, so one may consider increasing the order of PC expansion to improve the accuracy. This section will compare the accuracy between the PC expansion and the LHS-based statistical methods by using higher order expansion. The condition is considered to be the same case in the last subsection, but the geometries uncertainty is neglected to reduce the computational cost. As a result, there will be only 2 Gaussian random variables that are E_2 and E_3.

Using the PC expansion with order 4, 6, 9, 12, and 14 to estimate the dynamic response of the rigid-flexible multibody system, the corresponding sampling size is 25, 49, 100, 169, and 225. The LHS-based statistical method using the equivalent sampling size is also implemented. The reference solution is still produced by using the Monte Carlo method with 1000 samples. The error of the two methods changing with the sampling size is shown in Figs. 28 and 29.
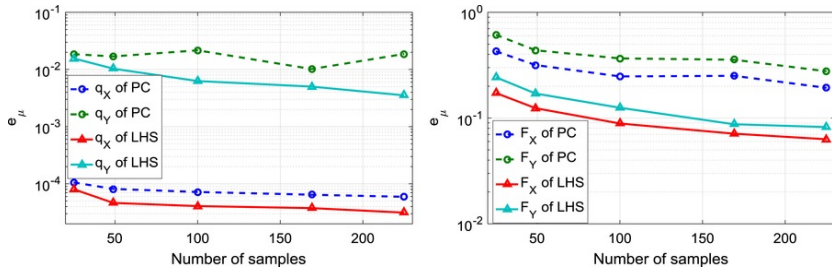

Fig. 28 The error of mean (larger sampling size).
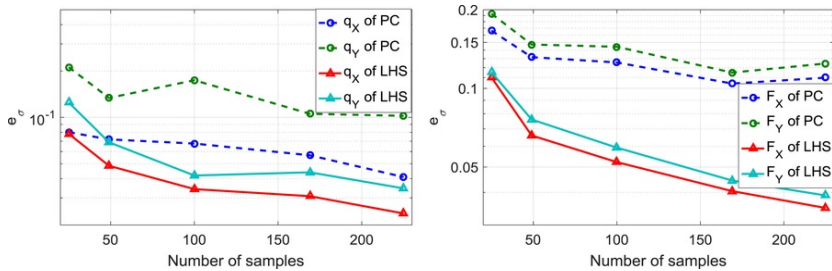
alt-text: Fig. 28

alt-text: Fig. 29

It can be found that the LHS-based statistical method shows higher accuracy than the PC expansion method when higher order expansion is used. Especially for estimating the response of the two reaction forces, even the PC expansion with order 14 (using 225 samples) is worse than the LHS-based statistical method with only 25 samples. Therefore, in this case the LHS-based statistical method shows better performance than the PC expansion method no matter what order of PC expansion is implemented.

To analyze the two methods in further, the univariate random variable is studied, which can show the shape of the responses with respect to the random variable clearly. 100 uniform samples of the random variable which has the largest effect to the responses will be selected, and other random variables will keep its mean value. For the long correlation length case, the random variable E_2 is sampled, and the random variable E_3 is sampled for the short correlation length case. Since the two random variables are standard Gaussian variables, they will be sampled from −3 to 3 with 100 uniform grids. For the long correlation length case, the model with high spring stiffness and damping ratio will be used to run the simulation, while the low spring stiffness and damping ratio model will be utilized to collect the responses for the short correlation length case.

The responses at 0.8 s under the long correlation case are shown in Fig. 30.
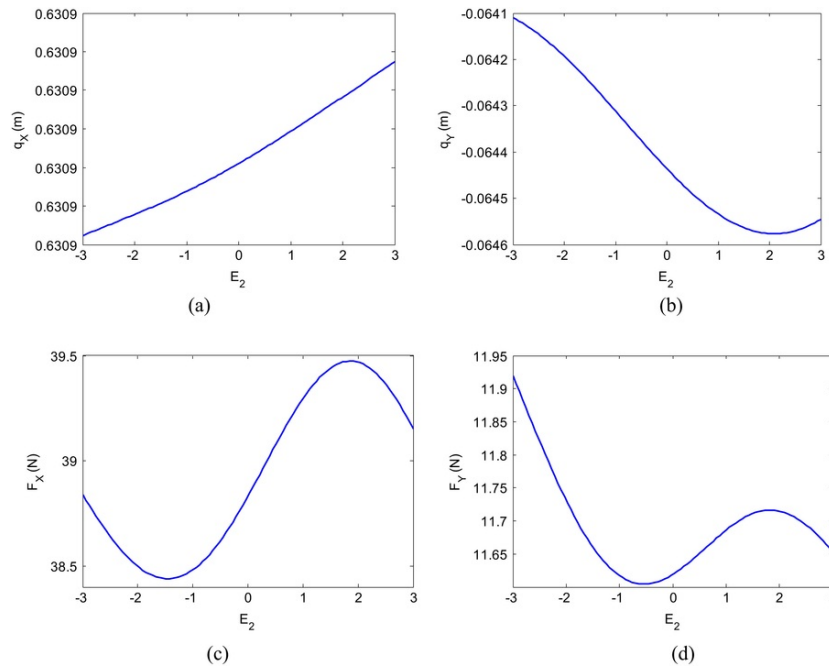

Fig. 30 Responses for the long correlation length case.

alt-text: Fig. 30

It can be found that all the four responses are quite smooth along the random variable E_2, no matter what the shape of these curves is. The accuracy of the PC expansion method is mainly determined by the accuracy of the Gaussian quadrature formula (Eq. (30)). For the smooth function, the Gaussian quadrature formula is usually highly accurate, which resulting the PC expansion method having quite good performance. Actually the LHS-based statistical method also has an acceptable accuracy in this case, but its stability is influenced by the randomness of the sampling points. On the other hand, the LHS-based statistical method still belongs to the Monte Carlo method, but its sampling points are specific. The convergence ratio of the Gaussian quadrature formula is higher than the Monte Carlo method for the low-dimensional smooth function, so the accuracy of the PC expansion method is higher than the LHS-based statistical method for this case.

Fig. 31 shows the responses at 0.8 s under the short correlation case. All the responses are non-smooth with respect to the random variable E_3. There are many high-frequency signals included in these responses, which will

leads to larger error in estimating the mean and standard deviation for both the PC expansion and LHS-based statistical methods. This is the reason that the accuracy for the case of short correlation length is lower than that of long correlation length case.
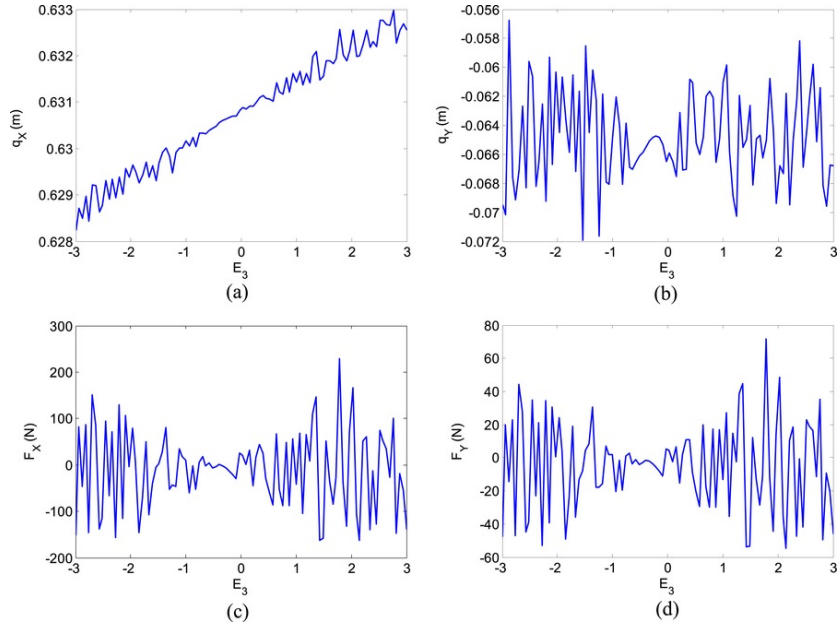

Fig. 31 Responses for the short correlation length case.

alt-text: Fig. 31

When there are many large magnitude high-frequency signals in the integrand, the accuracy of Gaussian quadrature formula decreases faster than the Monte Carlo method. As a result, the PC expansion method provides worse estimation than the LHS-based statistical method for most of the responses. Especially for q_Y, F_X, and F_Y, the magnitudes of the high-frequency signals are much larger than the magnitudes of the low-frequency signals. However, for q_X, the two methods give similar accuracy that is better than other 3 responses, because its magnitude of the high-frequency signals is smaller than that of the low-frequency signals.

In summary, for the smooth responses, the PC expansion method is more accurate and stable, because the Gaussian quadrature formula is highly accurate in this case. When there are many high-frequency signals with large magnitude contained in the responses, the LHS-based statistical method is better than the PC expansion method. Another issue should be mentioned is that the dimension of the random variables in this paper is not quite large (no larger than 3). When the dimensional size is quite large, the dimensional curse problem may reduce the performance of the PC expansion method. Hence, for high dimensional problems, the LHS-based statistical method should be recommended.

6 Conclusions

This paper investigates the dynamic responses of the rigid-flexible mechanisms under geometrical and material uncertainties. The deterministic model of the rigid-flexible multibody system is built by using the ANCF based method, in which the flexible parts are modeled by using ANCF elements, while the rigid parts are built by using the ANCF-RNs. The geometry uncertainty of rigid parts is modeled as uniform random variables, while the material uncertainty of flexible parts is modeled by a homogeneous Gaussian random field, which is further discretized to independent standard Gaussian random variables by using the EOLE method. Based on the generalized-**α** algorithm that is a deterministic solver for DAEs, the PC expansion and LHS-based statistical methods are introduced to estimate the mean and standard deviation of the system responses. From the analysis results of the slider-crank mechanism, it can be seen that the PC expansion method has higher accuracy and better stability for the smooth responses, while the LHS-based statistical method is better for the responses containing high-frequency and large-magnitude signals.

Acknowledgements

References

[1] A.A. Shabana, Computational Dynamics, 2001, John Wiley & Sons; New York.

[2] A.A. Shabana, Flexible multi-body dynamics review of past and recent developments, *Multibody Syst. Dyn.* **1**, 1997, 189–222.

[3] A.A. Shabana, An Absolute Nodal Coordinates Formulation for the Large Rotation and Deformation Analysis of Flexible Bodies, 1997, University of Illinois; Chicago.

[4] X. Du, P.K. Venigella and D. Liu, Robust mechanism synthesis with random and interval variables, *Mech. Mach. Theory* **44**, 2009, 1321–1337.

[5] A.A. Shabana, Dynamics of Multibody Systems, 2005, Cambridge University Press; New York.

[6] P. Eberhard and W. Schiehlen, Computational dynamics of multibody systems history, formalisms, and applications, *J. Comput. Nonlinear Dyn.* **60**, 2006, 489–511.

[7] Y. Zhang, Q. Tian, L. Chen and J. Yang, Simulation of a viscoelastic flexible multibody system using absolute nodal coordinate and fractional derivative methods, *Multibody Syst. Dyn.* **21**, 2008, 281–303.

[8] Q. Tian, Y. Zhang, L. Chen and J. Yang, Simulation of planar flexible multibody systems with clearance and lubricated revolute joints, *Nonlinear Dyn.* **60**, 2010, 489–511.

[9] K.S. Kerkkänen, D. García-Vallejo and A.M. Mikkola, Modeling of belt-drives using a large deformation finite element formulation, *Nonlinear Dyn.* **43**, 2006, 239–256.

[10] K. Dufva, K. Kerkkänen, L.G. Maqueda and A.A. Shabana, Nonlinear dynamics of three-dimensional belt drives using the finite-element method, *Nonlinear Dyn.* **48**, 2007, 449–466.

[11] J. Gerstmayr and A.A. Shabana, Analysis of thin beams and cables using the absolute nodal coordinate formulation, *Nonlinear Dyn.* **45**, 2006, 109–130.

[12] J. Gerstmayr, M.K. Matikainen and A.M. Mikkola, A geometrically exact beam element based on the absolute nodal coordinate formulation, *Multibody Syst. Dyn.* **20**, 2008, 359–384.

[13] Q. Tian, C. Liu, M. Machado and P. Flores, A new model for dry and lubricated cylindrical joints with clearance in spatial flexible multibody systems, *Nonlinear Dyn.* **64**, 2010, 25–47.

[14] C. Liu, Q. Tian and H. Hu, Dynamics of a large scale rigid–flexible multibody system composed of composite laminated plates, *Multibody Syst. Dyn.* **26**, 2011, 283–305.

[15] A.A. Shabana, ANCF reference node for multibody system analysis, *Proc. Inst. Mech. Eng., Part K: J. Multi-body Dyn.* **229**, 2014, 109–112.

[16] C. Liu, Q. Tian and H. Hu, Dynamics and control of a spatial rigid-flexible multibody system with multiple cylindrical clearance joints, *Mech. Mach. Theory* **52**, 2012, 106–129.

[17] J.C. Helton, J.D. Johnson, W.L. Oberkampf and C.B. Storlie, A sampling-based computational strategy for the representation of epistemic uncertainty in model predictions with evidence theory, *Comput. Methods Appl. Mech. Eng.* **196**, 2007, 3980–3998.

[18] J.Y. Dantan, N. Gayton, A.J. Qureshi, M. Lemaire and A. Etienne, Tolerance analysis approach based on the classification of uncertainty (Aleatory/Epistemic), *Procedia CIRP* **10**, 2013, 287–293.

[19] M. Beer, S. Ferson and V. Kreinovich, Imprecise probabilities in engineering analyses, *Mech. Syst. Signal Process.* **37**, 2013, 4–29.

[20] W. Gao, J.C. Ji, N. Zhang and H.P. Du, Dynamic analysis of vehicles with uncertainty, *Proc. Inst. Mech. Eng. Part D: J. Automob. Eng.* **222**, 2008, 657–664.

[21] C. Jiang, X. Han and G.P. Liu, A sequential nonlinear interval number programming method for uncertain structures, *Comput. Methods Appl. Mech. Eng.* **197**, 2008, 4250–4265.

[22] Z. Kang, Y. Luo and A. Li, On non-probabilistic reliability-based design optimization of structures with uncertain-but-bounded parameters, *Struct. Saf.* **33**, 2011, 196–205.

[23] Z. Qiu, Comparison of static response of structures using convex models and interval analysis method, *Int. J. Numer. Methods Eng.* **56**, 2003, 1735–1753.

[24] Z. Wang, Q. Tian and H. Hu, Dynamics of spatial rigid–flexible multibody systems with uncertain interval parameters, *Nonlinear Dyn.* **84**, 2016, 527–548.

[25] J. Wu, Z. Luo, Y. Zhang, N. Zhang and L. Chen, Interval uncertain method for multibody mechanical systems using Chebyshev inclusion functions, *Int. J. Numer. Methods Eng.* **95**, 2013, 608–630.

[26] D. Wu, W. Gao, C. Song and S. Tangaramvong, Probabilistic interval stability assessment for structures with mixed uncertainty, *Struct. Saf.* **58**, 2016, 105–118.

[27] J. Wu, Z. Luo, N. Zhang and Y. Zhang, A new uncertain analysis method and its application in vehicle dynamics, *Mech. Syst. Signal Process.* **50-51**, 2015, 659–675.

[28] D.M. Do, W. Gao and C. Song, Stochastic finite element analysis of structures in the presence of multiple imprecise random field parameters, *Comput. Methods Appl. Mech. Eng.* **300**, 2016, 657–688.

[29] W. Betz, I. Papaioannou and D. Straub, Numerical methods for the discretization of random fields by means of the Karhunen–Loève expansion, *Comput. Methods Appl. Mech. Eng.* **271**, 2014, 109–129.

[30] R.G. Ghanem and P.D. Spanos, Stochastic Finite Elements: A Spectral Approach, 1991, Springer-Verlag; New York.

[31] B. Sudret and A. Der Kiureghian, Stochastic Finite Element Methods and Reliability a State-of-the-art Report, 2000, University of Calnifornia; Berkeley.

[32] J. Zhang and B. Ellingwood, Orthogonal series expansion of random fields in reliability analysis, *J. Eng. Mech.* **120**, 1994, 2660–2677.

[33] C.C. Li and A. Der Kiureghian, Optimal discretization of random field, *J. Eng. Mech.* **119**, 1993, 1136–1154.

[34] S.S. Isukapalli, Uncertainty Analysis of Transport-transformation Models, 1999, The State University of New Jersey; New Brunswick, New Jersey.

[35] G.S. Fishman, Monte Carlo: Concepts, Algorithms, and Applications, 1996, Springer-Verlag; New York.

[36] M.D. Mckay, R.J. Beckkman and W.J. Conover, A comparison of three methods for selecting values of input variables in the analysis of output from a computer code, *Technometrics* **21**, 1979, 266–294.

[37] A.B. Owen, Orthogonal arrays for computer experiments, integration and visualization, *Stat. Sinca* **2**, 1992, 439–452.

[38] T.-T. Wong, W.-S. Luk and P.-A. Heng, Sampling with Hammersley and Halton Points, *J. Graph. Tools* **2**, 1997, 9–24.

[39] K.T. Fang, D.K.J. Lin, P. Winker and Y. Zhang, Uniform Design: Theory and Application, *Technometrics* **39**, 2000, 237–248.

[40] D. Xiu and G.E. Karniadakis, Modeling uncertainty in steady state diffusion problems via generalized polynomial chaos, *Comput. Methods Appl. Mech. Eng.* **191**, 2002, 4927–4948.

[41] D. Xiu and G.E. Karniadakis, Modeling uncertainty in flow simulations via generalized polynomial chaos, *J. Comput. Phys.* **187**, 2003, 137–167.

[42] L. Li and C. Sandu, On the impact of cargo weight, vehicle parameters, and terrain characteristics on the prediction of traction for off-road vehicles, *J. Terra.* **44**, 2007, 221–238.

[43] C. Sandu, A. Sandu and E.D. Blanchard, Polynomial chaos-based parameter estimation methods applied to a vehicle system, *Proc. Inst. Mech. Eng. Part K: J. Multi-body Dyn.* **224**, 2010, 59–81.

[44] J. Wu, Z. Luo, N. Zhang, Y. Zhang, Dynamic computation of flexible multibody system with uncertain material properties, Nonlinear Dyn., 2016.

[45] A. Sandu, C. Sandu and M. Ahmadian, Modeling multibody systems with uncertainties. Part I: theoretical and computational aspects, *Multibody Syst. Dyn.* **15**, 2006, 369–391.

[46] C. Sandu, A. Sandu and M. Ahmadian, Modeling multibody systems with uncertainties. Part II: numerical applications, *Multibody Syst. Dyn.* **15**, 2006, 241–262.

[47] A. Sarkar and R. Ghanem, Mid-frequency structural dynamics with parameter uncertainty, *Comput. Methods Appl. Mech. Eng.* **191**, 2002, 5499–5513.

[48] D. Lucor, C. Enaux, H. Jourdren and P. Sagaut, Stochastic design optimization: application to reacting flows, *Comput. Methods Appl. Mech. Eng.* **196**, 2007, 5047–5062.

[49] E. Jacquelin, M.I. Friswell, S. Adhikari, O. Dessombz and J.J. Sinou, Polynomial chaos expansion with random and fuzzy variables, *Mech. Syst. Signal Process.* **75**, 2016, 41–56.

[50] D. García-Vallejo, J. Mayo, J.L. Escalona and J. Domínguez, Three-dimensional formulation of rigid-flexible multibody systems with flexible beam elements, *Multibody Syst. Dyn.* **20**, 2008, 1–28.

[51] J.T. Sopanen and A.M. Mikkola, Description of elastic forces in absolute nodal coordinate formulation, *Nonlinear Dyn.* **34**, 2003, 53–74.

[52] J. Garcia De Jalon, J.L. Escalona, J. Mayo and J. Domínguez, Describing rigid–flexible multibody systems using absolute coordinates, *Nonlinear Dyn.* **34**, 2003, 75–94.

[53] D. García-Vallejo, J. Mayo, J.L. Escalona and J. Domínguez, Efficient evaluation of the elastic forces and the jacobian in the absolute nodal coordinate formulation, *Nonlinear Dyn.* **35**, 2004, 313–329.

[54] Q. Tian, L.P. Chen, Y.Q. Zhang and J. Yang, An efficient hybrid method for multibody dynamics simulation based on absolute nodal coordinate formulation, *J. Comput. Nonlinear Dyn.* **4**, 2009, 021009.

[55] M. Arnold and O. Bruls, Convergence of the generalized-α scheme for constrained mechanical systems, *Multibody Syst. Dyn.* **18**, 2007, 185–202.

[56] E. Vanmarcke, Random Fields Analysis and Synthesis, World Scientific, Singapore, 2010.

[57] R.-B. Chen, D.-N. Hsieh, Y. Hung and W. Wang, Optimizing Latin hypercube designs by particle swarm, *Stat. Comput.* **23**, 2012, 663–676.

[58] P.Z.G. Qian, Sliced latin hypercube designs, *J. Am. Stat. Assoc.* **107**, 2012, 393–399.

[59] F.A.C. Viana, G. Venter and V. Balabanov, An algorithm for fast optimal Latin hypercube design of experiments, *Int. J. Numer. Methods Eng.* **82**, 2009, 135–156.

[60] M. Abramowitz and I.A. Stegun, Handbook of Mathematical Functions with Formulas, Graphs, and Mathematical Tables, 1972, Dover; New York.

Highlights

- Firstly investigate the random uncertainty in analyzing the dynamic responses of the rigid-flexible multibody systems.
- The combination of random variables and random field to describe the geometry of rigid bodies and material properties of flexible bodies.
- PC expansion method, LHS-based statistical method, and the ANCF-based modelling method are systematically integrated to solve the dynamics equations of rigid-flexible multibody systems with random variables.

Queries and Answers

Query:

Your article is registered as a regular item and is being processed for inclusion in a regular issue of the journal. If this is NOT correct and your article belongs to a Special Issue/Collection please contact s.padmanabhan@elsevier.com immediately prior to returning your corrections.

Answer: Correct.

Query:

Highlights should only consist of 85 characters per bullet point, including spaces. The highlights provided are too long; please edit them to meet the requirement.

Answer: 1.Random uncertainty analysis in the rigid-flexible multibody systems.
2.Combination of random variables and random field for describing uncertainty.
3.Systematically integration of PCE, LHS, and the ANCF methods.

Query:

Please note that Refs [31] and [34] were identical, and Ref. [34] has been deleted. The subsequent references have been renumbered. Kindly approve changes.

Answer: The change is correct.

Query:

Please validate the inserted journal title for Ref. [52].

Answer: Nonlinear Dynam